Westinghouse ENGINEER

NOVEMBER 1963

1

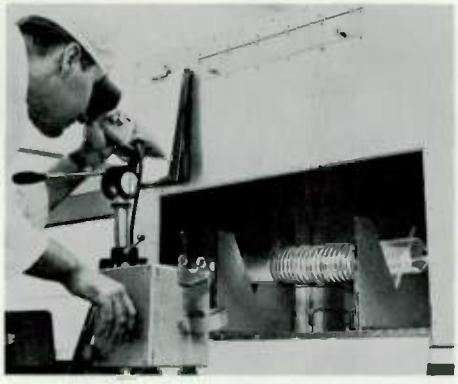

2

3

4

5

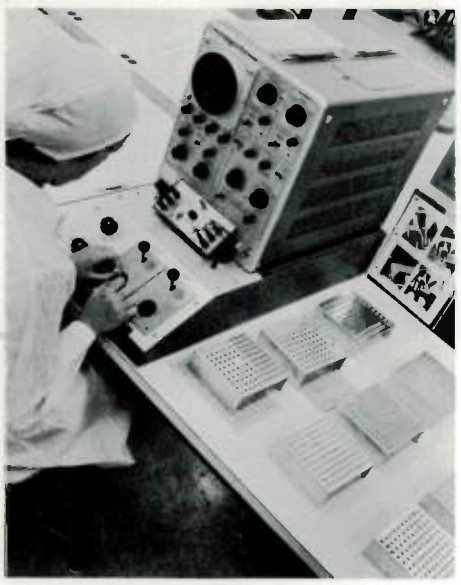

(*1*) An optical pyrometer is used to take a temperature profile during an epitaxial growth operation. (*2*) Masking slides are produced with a tolerance equal to only a fraction of the width of a hair. The operator is mounting a pattern that will be photographed and reduced from several square feet to about the size of a pinhead. As many as 150 copies of this reduced pattern are reproduced on a single plate about the size of a quarter. (*3*) A silicon wafer, which has been coated with a photosensitive material, is exposed to light causing portions of the photosensitive material to harden, and leaving the shaded portions in a condition for further processing. (*4*) Silicon dice, or chips, as small as 0.05 inch square are mounted into transistor packages. (*5*) After mounting and prior to encapsulation, integrated circuits are checked for voltage-current characteristics and for proper connections.

Molecular Electronics—from Laboratory to Mass Production

Tiny electronic circuits, barely discernible to the eye, are now the focus of attention in the $4-billion electronic components industry in the United States. This new art of molecular electronics, also called integrated circuits, has reached the initial stages of mass production. Shown here are scenes from a new Westinghouse plant near Baltimore, which consolidates molecular electronic activities that had been carried on in laboratories in several other locations. Because of the cleanliness required in the manufacturing process, the entire plant is practically one large clean room. Employes in production, engineering, and development areas wear dust-free, lint-free white coats and caps, giving most of the plant the look of a hospital.

The new technology has brought about major size and weight reductions in electronic circuitry, greater reliability and improved performance. Complete functions that normally require as many as 50 electronic components can be performed within a single tiny block of solid material. As many as 150 separate but identical electronic circuits are made at one time on a silicon wafer about the size of a quarter. The circuits are then "diced" and placed in individual packages.

At Westinghouse, integrated circuits are manufactured by an "epitaxial diffused planar process." The starting material is a silicon wafer 5 to 10 mils thick. Additional layers of silicon-substrate are formed on some of the blocks by a vapor growth process. The wafer is then masked with a layer of oxide, and transistor junctions, diodes, and resistive and capacitive areas are formed in the silicon substrate by successively opening windows in the oxide with photomasking techniques, and driving impurities through these windows by gaseous diffusion.

The silicon wafer is untouched by hand from start to finish of the process. Because of the tiny size of circuits and the high precision required, most of the manufacturing processes require handling under microscopes with high magnification.

Westinghouse
ENGINEER

Cover Design: The UK-2/S-52 satellite carries instrumentation to measure galactic noise, vertical distribution of upper atmospheric ozone, and the size and number of micrometeoroids in the ionosphere. Thomas Ruddy, of Town Studios, Pittsburgh, illustrates the satellite on this month's cover.

Published bimonthly by the Westinghouse Electric Corporation, Pittsburgh, Pennsylvania.
Subscriptions: United States and Possessions, $2.50 per year; all other countries, $3.00 per year; single copies, 50¢ each.
Mailing address: Westinghouse ENGINEER, P.O. Box 2278, 3 Gateway Center, Pittsburgh, Pennsylvania 15230.
Microfilm: Reproductions of the magazine by years are available on positive microfilm from University Microfilms, 313 North First Street, Ann Arbor, Michigan.
Printed in the United States by The Lakeside Press, Lancaster, Pennsylvania.

NOVEMBER 1963 VOLUME 23 / NUMBER 6

The UK-2/S-52 International Satellite Program

Emil W. Hymowitz, *Project Manager, National Aeronautics and Space Administration, Goddard Space Flight Center, Greenbelt, Maryland.*

Harold M. Watson, *Project Manager, Air Arm Division, Westinghouse Electric Corporation, Baltimore, Maryland.*

This joint United States-United Kingdom project will provide new information on galactic noise, ozone distribution in the atmosphere, and the quantity and size of micrometeoroids in space.

The S-52 satellite is the second of three scientific satellites in the cooperative international program being conducted by the United Kingdom and the United States. British scientists in university and government laboratories have designed and constructed the instrumentation for the S-52 experiments under the scientific direction of the British National Committee for Space Research; British scientists also will reduce and analyze all data gathered from the spacecraft. The Office of the Minister for Science has overall administrative responsibility for the U. K. program.

The Goddard Space Flight Center, for NASA, has overall U. S. responsibility for the program, including design, development, construction, and testing of the spacecraft as well as the launching, tracking and data acquisition phases. The Goddard Space Flight Center is also designing and providing certain subsystems. GSFC has contracted to Westinghouse the design and manufacture of some of the satellite subsystems, and the integration of all subsystems into an operating satellite. Westinghouse engineers will also assist in environmental proof testing of completed satellites.

Environmental tests of completed satellites are being performed now by U. K. scientists, and by Westinghouse and Goddard personnel at the Goddard Space Flight Center's environmental testing complex in Greenbelt, Maryland.

The NASA Langley Research Center is responsible for the launch vehicle system. Launching will take place at Wallops Island, Virginia, during 1963 utilizing an Advanced Scout vehicle.

The spacecraft structure will be a modified version of the UK-1/S-51, with a diameter of approximately 23 inches and a weight limit of 150 pounds. The structure is basically two honeycomb decks coupled by a center tube to the separation mechanism. The lower deck and appendages are braced by several struts between the lower deck bottom and the center tube. The outer shell of the satellite, made of fiberglass, completes the structure support and serves as the thermal coating surface and ground plane.

The unit will have a spin rate in orbit of 5 rpm after a de-spin sequence from a spin of 160 rpm. The de-spin mechanism consists of two weighted cables wrapped around the outer skin of the satellite between the two decks. When the weights are released, the unwrapping of the cables causes the satellite (and fourth stage) to de-spin from the initial spin rate of 160 rpm down to approximately 80 rpm. The erection of booms, paddles, and antenna deployment further de-spins the satellite to the final spin rate of approximately 5 rpm.

Experimental Program

The satellite will be launched into an orbit with an apogee of approximately 800 nautical miles, a perigee of approximately 150 miles, at an inclination of 51 degrees. The purpose of the spacecraft is to carry instrumentation for the three following experiments:

Galactic Noise—This experiment is designed to measure the radio frequency signals generated by stars and galaxies in the frequency range from 0.75 to 3.0 megacycles. This information is of primary value to radio astronomers, who have little information on galactic noise in this frequency range because of the opacity of the ionosphere. The galactic noise experiment will be furnished by the Mullard Radio Astronomy Observatory, Cavendish Laboratory, University of Cambridge, under the supervision of Dr. F. Graham Smith.

Measurements will be made with a 130-foot dipole antenna and two ferrite rod antennas. Immediately after separation from the fourth stage vehicle, the 130-foot dipole antenna (65 feet on each side) will be deployed from a drum through two booms on either side of the satellite. Centrifugal force will pull the wire through the boom from

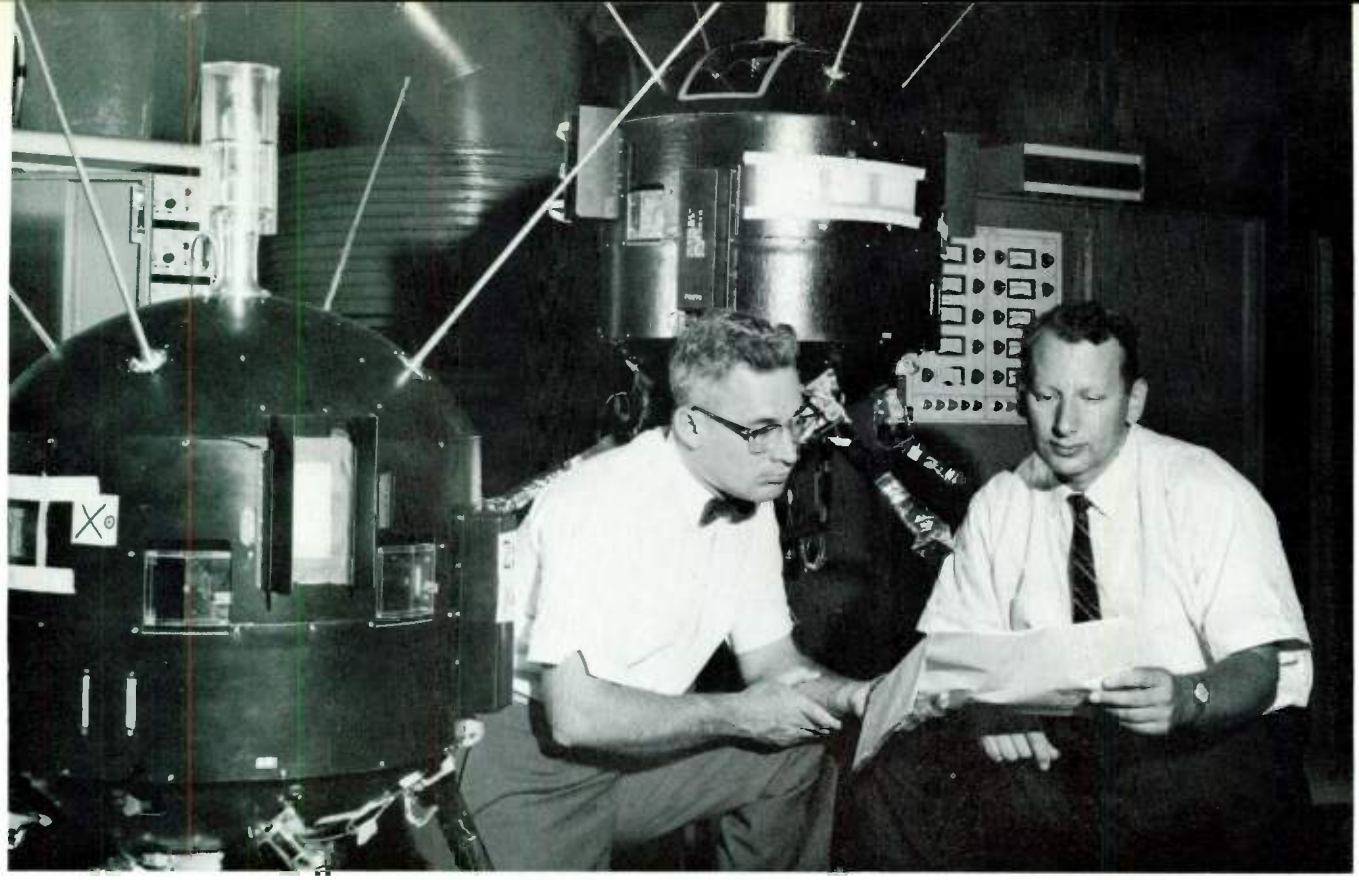

UK-2/S-52 FLIGHT 1 SATELLITE (*left*) and the prototype satellite are shown being prepared for tests at the Goddard Space Flight Center at Greenbelt, Maryland. The Flight 1 satellite, which will be orbited, is shown as it is about to go into the thermal vacuum chamber for flight acceptance tests. The prototype is being readied for an additional solar simulation test.

1

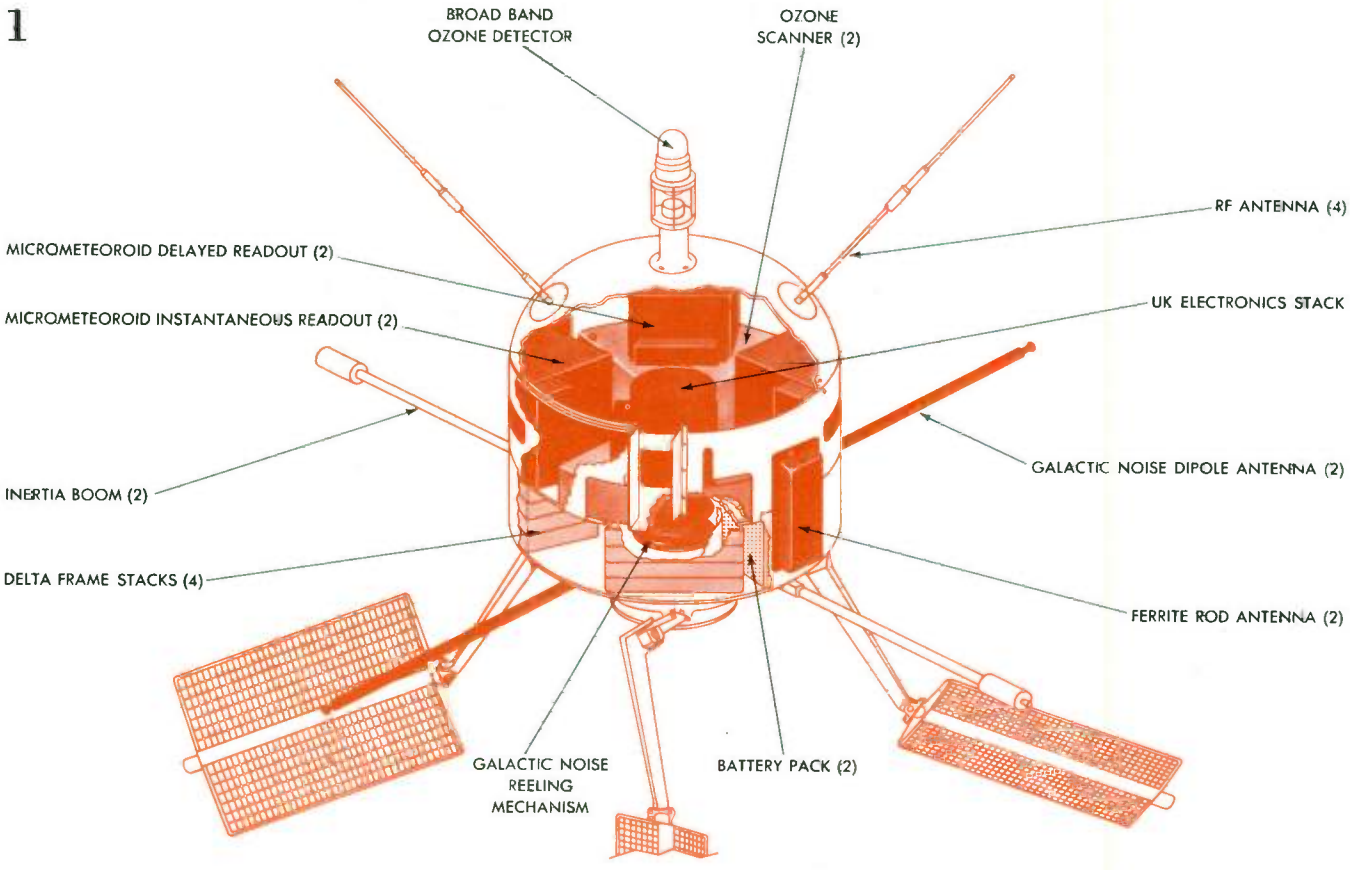

FUNDAMENTAL COMPONENTS of the satellite are located on an upper and lower deck.

2

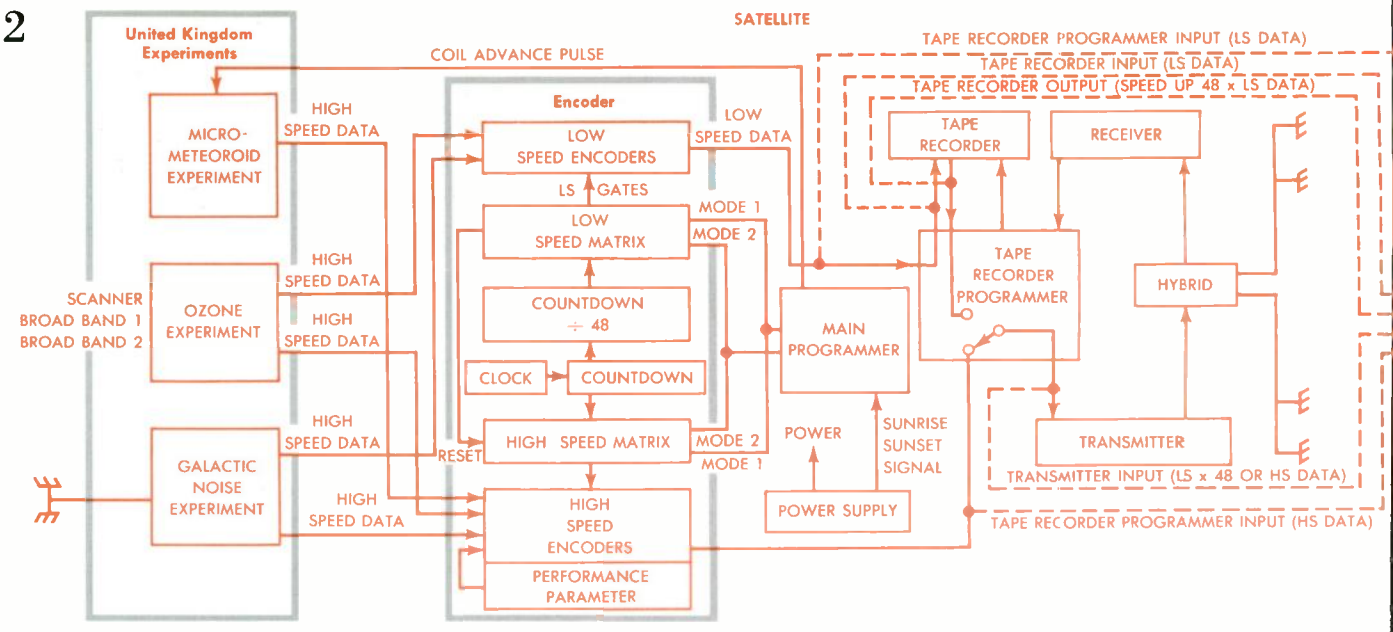

the drum, which will be held at a constant speed by a motor drive mechanism.

The two ferrite loops are mounted on diametrically opposite sides of the satellite and will be tuned to approximately two megacycles. These antennas will provide useful data even if the dipole antennas fail to deploy.

Galactic noise will be measured from both antennas as the receiver sweeps repeatedly over the range of 0.70 to 3 megacycles.

Atmospheric Ozone—The second experiment will measure vertical distribution of ozone in the upper atmosphere by two techniques: a broadband method and spectrum scanning method. Although ozone distribution in the lower atmosphere is regularly probed by rocket soundings, little data is available for the upper region. This information is desired by meteorologists because it is believed to be related to the heat balance of the earth. The experiment is supplied by the U. K. Air Ministry, Meteorological Office, under the supervision of Dr. K. H. Stewart.

The broadband measurement method uses a simple photocell with a spectral response of 1800 to 3500 angstroms. In this region, most atmospheric attenuation is due to ozone. Therefore, during satellite "sunrise" and "sunset," when the satellite is illuminated by sunlight passing through the atmosphere, photocell output indicates the amount of ozone present by virtue of the spectral energy absorbed.

Because some attenuation is caused by dust and air molecules, a second photocell is needed in the broadband unit to determine this effect. The second photocell response is 3600–4000 angstroms; output of this photocell is

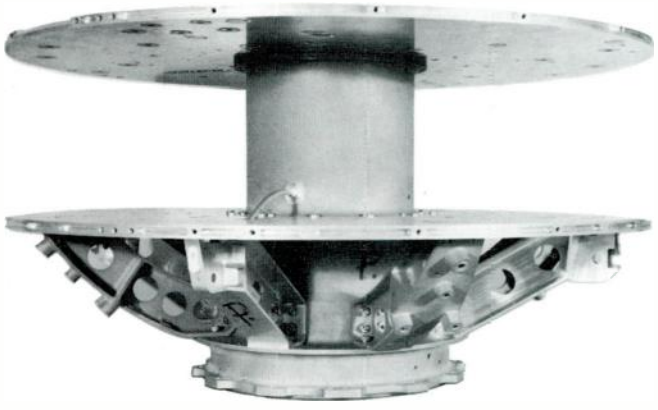

BASIC SATELLITE STRUCTURE (*right*) **consists of a center tube, an upper and lower deck, and strengthening struts on the lower deck to support appendages.**

ELECTRONIC EQUIPMENT for the satellite subsystems is packaged in standardized delta packs (*below*), **which are mounted in frames on the lower deck (Fig. 1). Because of the high-density packaging, and to gain reliability, submodules and delta pack cards use welded terminal construction techniques. These three packs comprise the telemetry encoder subsystem.**

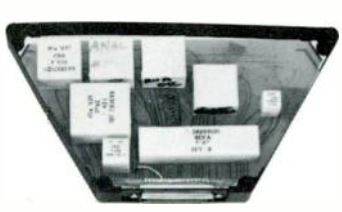

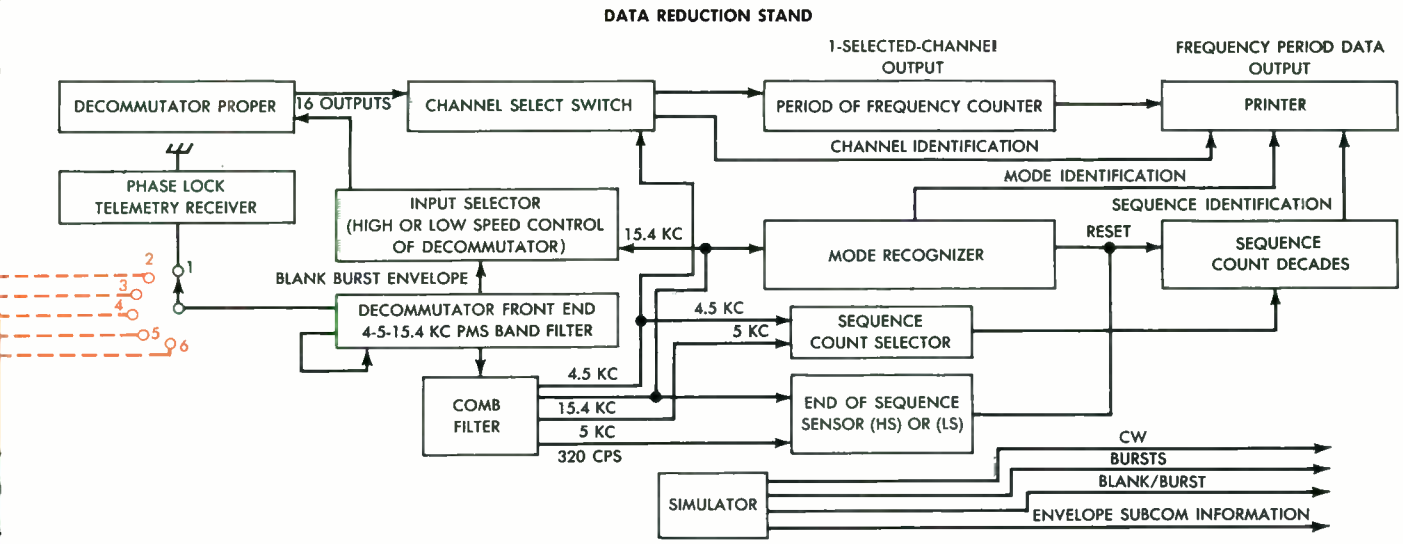

SATELLITE SUBSYSTEMS and the data reduction stand are shown in this block diagram; the data reduction stand, for testing the satellite subsystems, is intercoupled to the satellite through both umbilical connections and the r-f telemetry link.

used to correct the information obtained from the other photocell, so that a true measure of ozone concentration is obtained.

The spectrometer method of measuring ozone uses a simple form of prism spectrometer to scan through the solar spectrum in the 2650–4000 angstrom region. Scanning is accomplished by satellite rotation. As the satellite rotates, each of eight optical units in turn causes the solar spectrum to scan across one of two photomultiplier units. The shape of each of the pulses of light received by the photomultipliers corresponds to the shape of the solar spectrum as modified by ozone absorption.

Micrometeoroid Flux—The third experiment is designed to measure the size and number of micrometeoroids in the ionosphere. Micrometeoroids, ranging in size from a grain of sand down to millionths of an inch, cause an eroding effect on spacecraft. The information gained will be useful in the design of future spacecraft and space stations. The experiment will be supplied by the Nuffield Radio Astronomy Laboratories, University of Manchester, under the supervision of Dr. R. C. Jennison.

Two pairs of micrometeoroid detectors will be used. One pair are called *instantaneous read-out detectors* and the other pair, *delayed read-out detectors*.

The instantaneous read-out detectors (or IROD units) determine the size and quantity of micrometeoroids by measuring the light admitted through punctures in an aluminum foil. The punctures are made by micrometeoroids as they impact on the exposed foil, which is advanced across the aperture of the IROD unit. The foil is coiled on a spool and is advanced approximately 1/16 inch every other orbit. Light admitted through the punctures is sensed by solar cells within the unit.

The delayed read-out detectors (or DROD units) are primarily designed to measure the erosion effects of very small micrometeoroids. In this case, the light admitted through abrasions on a metalized Mylar surface is measured. The metallic coating on the Mylar is only about 5 microns thick. The Mylar is coiled on a spool and advanced across an aperture, similar to the IROD unit.

Satellite Subsystems

In addition to the instrumentation required for the three experiments, several additional subsystems are required to provide supporting functions in gathering and transmitting experimental data to earth.

Programmer Subsystem—All systems within the satellite are supervised by a programmer subsystem supplied by GSFC, which issues commands for sequencing the various events, such as: Commanding low- and high-speed encoders, advancing the foil in the micrometeoroid experiment, gating encoder channels, providing a sunrise identification signal, operating the tape recorder, initiating the under-voltage cut-off signal, and one-year timer cutoff. The one-year timer is required to shut off the satellite transmitter at the conclusion of the space experiment and free the carrier frequency band for other uses.

Telemetry Encoder Subsystem—This subsystem consists of high- and low-speed encoders that accept experiment output signals, commutate them, and convert them to a frequency proportional to the value of each parameter being measured in each of the experiments.

The output of the high-speed encoder modulates the transmitter output directly; the output of the low-speed encoder is recorded on a tape recorder, which plays back the data at 48 times recorder speed for transmitting.

Transmitter-Receiver Subsystem—The telemetry system of the S-52 uses a pulsed-frequency modulation system (PFM). The transmitter relays the encoder output and tape-recorded information (on command) to ground tracking stations. The satellite receiver monitors the ground command to switch the tape-recorded data into "playback" through the transmitter. This subsystem was designed by GSFC.

Power Supply Subsystem—The power supply subsystem provides power to the various electronic packages at ten

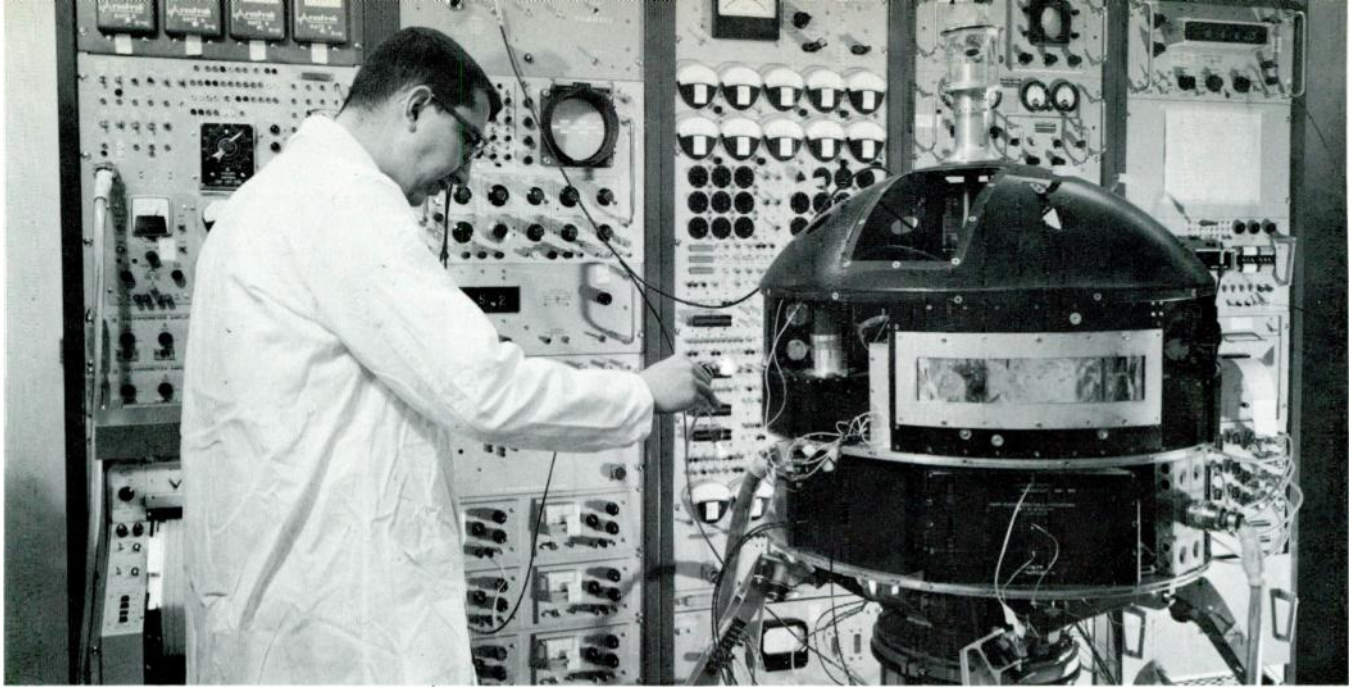

PROTOTYPE SATELLITE is shown during integration of subsystems. This unit will be exposed to all environmental tests.

levels of dc voltage and one level of ac voltage, in addition to the basic battery bus voltage. Solar paddles are the basic source of power, and they must supply the load and charge the batteries during the daylight portion of the orbit. During darkness, the batteries supply the load.

Four solar paddles are mounted on the ends of hinged arms attached to the lower deck struts. Originally, P-on-N type cells were selected, but because of the performance degradation expected by the enhanced (artificial Van Allen) radiation belt, a change was made to the more radiation-resistant N-on-P cells.

Two battery packs are mounted on the lower deck. Each pack contains 11 nickel-cadmium cells. The batteries are highly reliable and intended to support a minimum satellite life of one year. Only one battery is operational; the second is a reserve unit.

Engineering a Satellite

The integration of all satellite system elements has been by an orderly step-by-step procedure to insure that all satellite components are operational and electrically and physically compatible. A thorough testing procedure will assure flight readiness.

Two structural satellite models, a prototype satellite, and designated subsystems are being subjected to rigorous qualification testing. The structural models, called the *engineering test unit* and the *dynamic test unit*, were used in early structure tests. The dynamic test unit was built to test the deployment of all appendages, which are tied down to the outer casing of the Scout fourth stage during launch and must be released to assume their natural orbiting position. To test deployment, the dynamic test unit was mounted on a spin-up fixture in a vacuum chamber and actual de-spin sequence conditions were simulated.

The engineering test unit was exposed to various environmental conditions, such as vibration and acceleration, to evaluate the structural integrity of the satellite.

The prototype satellite will be exposed to the same tests as the structural models, plus thermal-vacuum, temperature, and humidity tests. The flight model satellite will be exposed to thermal-vacuum and vibration tests of a level commensurate with actual flight conditions.

Test Stand and Data Reduction Systems—Two test stand and data reduction systems have been constructed for this program. This unit couples into the satellite through umbilical connections, and through the r-f telemetry link. The system permits satellite equipment to be completely operated and evaluated. Data reduction is an important provision of the unit, since it allows quick evaluation of the data received from the satellite. A block diagram of the principal elements of the satellite and the data reduction stand and their intercoupling is shown in Fig. 2.

Reliability

Many man-years of engineering effort have gone into the development of this small, scientific satellite. And this effort is independent of that required for the launch vehicle and associated launch facility.

Considerable experience has been gained in designs of this type of satellite over the past five years; therefore, the primary problems that plague the satellite designer are those of selecting an optimum design for the desired satellite lifetime—in this case, about one year. But the problem of proving subsystem reliability is a difficult one. The reliability mechanism is not completely understood, and even if it were, reliability probably could not be completely controlled. It is therefore desirable that: (1) Designs should be extremely conservative; (2) several models of the final design should be placed on realistic life test as early as possible; and (3) prototype models of the final design should be subjected to considerable mechanical, electrical, and environmental overtest to bring out potential modes of equipment failure. This is the pragmatic approach to reliability; reliability studies are useful in choosing designs and components, but only rigorous testing provides confidence of trouble-free performance for long periods of time. This has been the approach to the development of the S-52 satellite.

Adjustable-Frequency Power Inverter Systems for Industry

C. G. Helmick, *Industrial Systems,*
Westinghouse Electric Corporation, Pittsburgh, Pennsylvania.
K. Lipman, *General Control Division,*
Westinghouse Electric Corporation, Buffalo, New York.

Solid-state inverter systems maintain set frequency with unexcelled accuracy. The one described here also provides inherent service continuity and an output wave form with little harmonic distortion.

Many process industries depend on adjustable-frequency ac power for coordinated control of groups of simple and inexpensive ac motors over a wide speed range. With the processes becoming increasingly complex and the control requirements increasingly stringent, these industries have been looking for an adjustable-frequency power supply that is simpler, more reliable, and more precise than the rotating frequency converters that have commonly been used.

In the production of man-made fibers, for example, slight variations in motor speeds caused by line fluctuations or load disturbances can spoil the product or cause it to be downgraded. Variations only slightly greater can break all the strands of yarn on a machine, causing several hours of lost production. Even more serious, process materials may undergo irreversible chemical changes if the electrical system fails, resulting in very high loss due to lost time and damaged equipment.

Reliable fixed-frequency inverters, with transistors or controlled rectifiers as switching elements, were developed some time ago for electronic applications. Improvements in controlled rectifiers, such as large power-handling capability and extremely fast turn-on and turn-off time, then stimulated much effort toward development of wide-range adjustable-frequency inverters for motor drive systems. The basic approach in most cases was to modify the constant-frequency inverters that had been designed for electronic equipment.

However, a motor system is not at all like an electronic load, so the initial marriage was not a good one. Most electronic loads are passive, while a motor load has a very real and active counter emf. Furthermore, a motor invariably operates with a lagging power factor, requiring the switching of large amounts of reactive current. To make matters more difficult, loads can switch quickly from motoring (demanding energy from the power source) to regenerating (requiring the source to absorb energy). All of these factors posed problems in building inverter drive systems.

Development engineers at the Aerospace Electrical Division achieved a breakthrough in inverter technology in 1961 with a system that provided harmonic neutraliza-

1

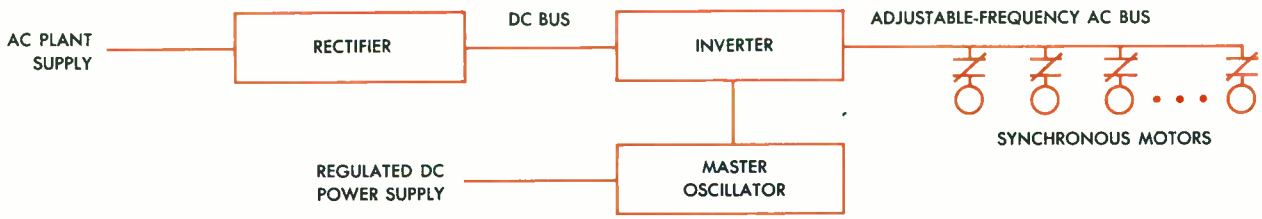

A SINGLE-INVERTER SYSTEM operates from constant-potential dc power and supplies adjustable-frequency ac power to the loads. If the loads are synchronous motors, all operate at exactly the same speed, and the speeds of all can be changed in unison by changing frequency. The inverter's output frequency is controlled by a master oscillator.

2

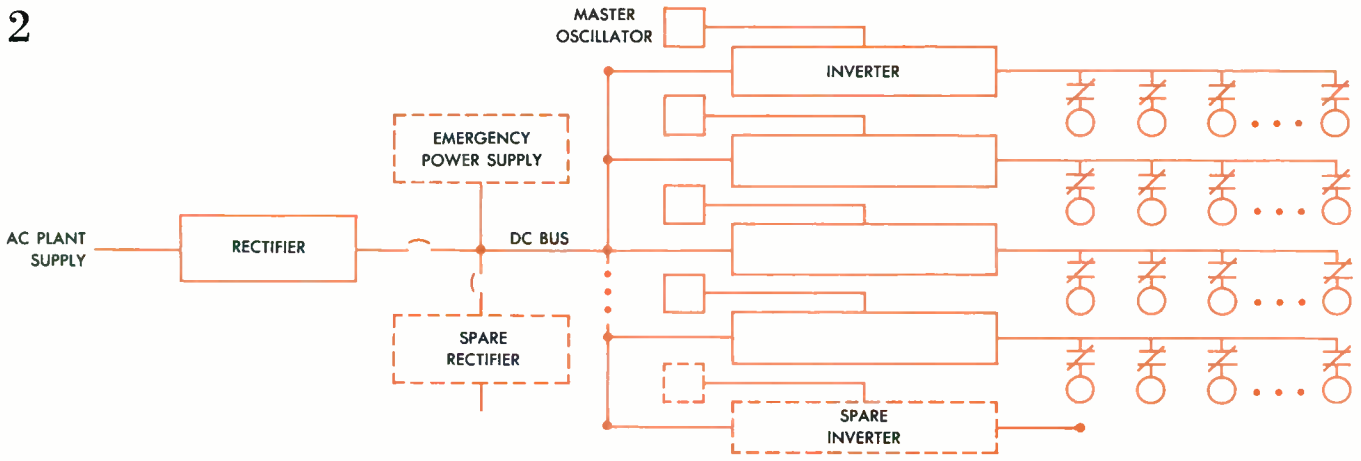

A MULTI-INVERTER SYSTEM is used for processes that require several groups of motors with independent speed control. This arrangement permits regenerated power to be returned to the dc bus. The adjustable-frequency inverters can be operated from a single dc power supply. A spare rectifier, spare inverter, and emergency power supply can be included.

3

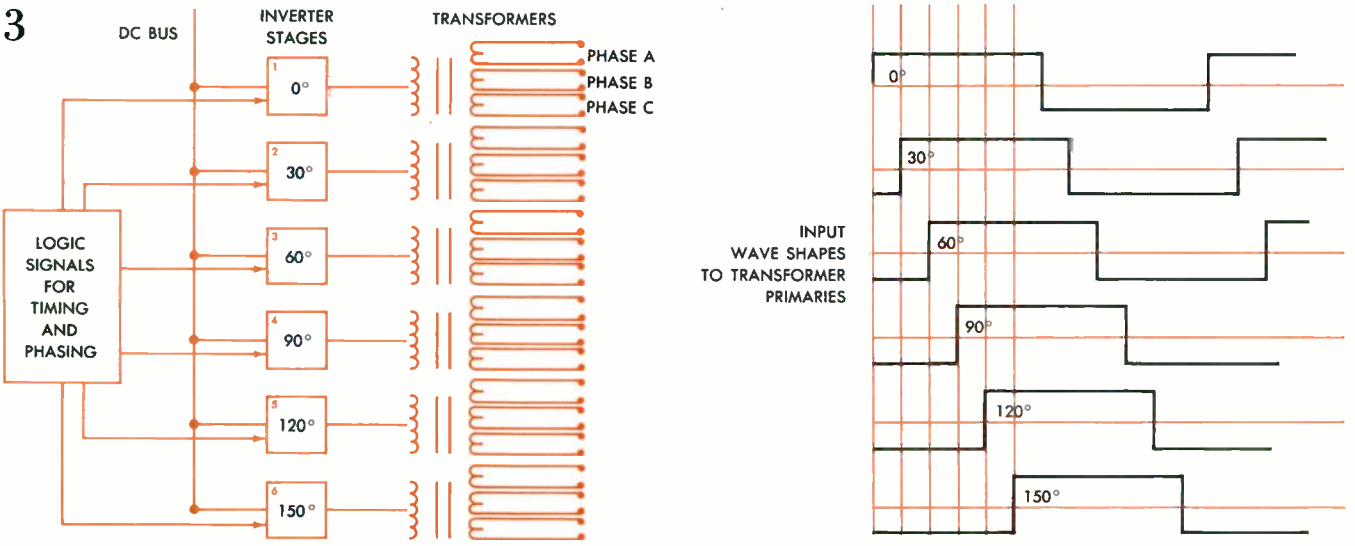

SIX OR MORE IDENTICAL STAGES energized from a dc supply are used in the Accur/Con 200 power inverter system. Each stage is a single-phase inverter producing a square-wave output. Each stage's output wave is delayed by 30 degrees from that of the preceding stage. The output of each stage is connected to a transformer that has three secondary windings.

4a b c

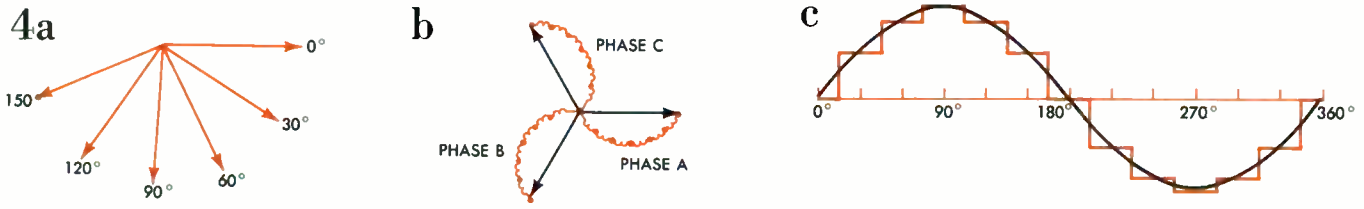

A THREE-PHASE WAVE IS PRODUCED by adding the outputs of the transformer secondaries. (*a*) Delaying the successive outputs of the inverter stages as shown in Fig. 3 results in a series of output voltages. (*b*) These voltages, transformed by the three transformer secondaries in each stage, are combined by vector addition to provide a three-phase output. Each secondary winding in a stage is connected in a different phase of the three-phase output. (The windings are displaced here to illustrate their vector relationships to each other.) (*c*) The result is a balanced set of three-phase voltages. Each phase's voltage wave is a multistepped wave approximating the ideal sine wave, with the major harmonics cancelled by the transformer connections.

tion, an effect that will be described shortly. The system appeared to offer great potential, so the General Control Division set out to adapt the basic work to adjustable-frequency inverters for the burgeoning process industries. The design objectives included:

Precise frequency control with long-term stability;
Reliability, to avoid shutdown even with a component failure;
Wide range of frequency control;
Simple voltage control to meet the requirements of motors for constant volts per cps;
Output waveshape with minimum harmonic distortion;
Simple and reliable commutation, or switching, of the controlled rectifiers under all conditions of operation;
Operation of several inverters from a single dc supply to permit use of a single large rectifier for low unit cost;
Electrical isolation between power input and power output and between inverters, for flexibility in safety and grounding practices;
Ease of servicing, and simple trouble-shooting procedures;
Flexibility of operation by manual control, remote control, automatic programming signals, or computer commands;
High conversion efficiency and low operating cost;
Economical use of floor space.

The result is the Accur/Con 200 power inverter system that is described in this article. First, however, consider some ways in which inverter drive systems can be used in industry.

Inverter Drive System Arrangements

Single-Inverter System—A system with a single adjustable-frequency power inverter is diagrammed in Fig. 1. A simple unregulated rectifier provides constant-potential dc power. The inverter switches the dc power to an ac output at a frequency determined by the switching rate, which is controlled by a separate master oscillator. Since the inverter is essentially a synchronous switch, it can switch only at the rate determined by the master oscillator. This master oscillator is isolated from the load and power supply, so it is not affected by load disturbances and power-supply fluctuations.

The master oscillator is made precise by careful design and by protection from temperature variations. Therefore, the output frequency of the power inverter is also extremely constant, and all synchronous motors connected to it operate at the same speed. The oscillator frequency is adjusted to change inverter frequency and thereby change motor speed.

No harm is done if the motors are overhauled by the load and caused to regenerate power. The regenerated power goes back smoothly through the inverter, which acts as a rectifier in this direction. This energy must have a place to go, however. With a single inverter supplied from a single rectifier, some means such as a dynamic braking resistor is provided to absorb the regenerated energy. Regenerative control circuitry automatically connects the resistor bank across the dc line during power feedback. It is designed to make the most economical use of the resistor bank by keeping it from bleeding power from the dc supply under normal operating conditions.

Multi-Inverter Systems—For some processes, several inverters can be operated advantageously from a single dc bus as diagrammed in Fig. 2. Each group of motors is supplied from its own inverter and master oscillator, so each group can be controlled independently. An additional advantage is that a single large rectifier can be used for all inverters in the plant, thereby reducing the unit cost of the dc supply.

Also, a single stand-by power supply on the dc bus can provide continuity of power during momentary ac power interruptions. This stand-by source may be a station battery or motor-generator set. Without it, dc voltage would be lost if ac power were interrupted momentarily. The adjustable-frequency voltages produced by the several inverters would then decay rapidly, limited only by the energy-storage capabilities of the circuit elements. (In general, this is 5 to 10 cycles of 60-cycle power.) Restoration of ac power could cause sufficient inrush current to blow all the protective fuses in the inverters.

Another advantage of a multi-inverter system is that it can utilize regenerated power. Suppose, for example, that the motors of one section in Fig. 2, say a tension holdback section, are overhauled by the load and caused to regenerate power. The power goes back through the inverter to the dc bus, where it helps carry the load on the rectifier.

The Accur/Con 200 Inverter System

Design—The Accur/Con 200 system is an inverter composed of a number of identical stages, typically six, connected to a dc supply as shown in Fig. 3. Each stage is a basic single-phase inverter, producing a square-wave single-phase output voltage. The output of each stage is connected directly to a single-phase transformer that has three secondary windings.

The problem is to construct a balanced three-phase set of voltages from the six single-phase outputs of the inverter stages. This is accomplished partly by proper timing and phasing of the switching signals applied to each power stage. These signals are supplied by a logic system that distributes the pulses from the master oscillator to cause the silicon controlled rectifiers to conduct in the desired sequence and for the proper length of time. For example, if stage 1 is considered as a reference, then the logic signals applied to stage 2 are delayed by 30 degrees, those applied to stage 3 by 60 degrees, and so on. The result is a series of output voltages (Fig. 4).

The rest of the solution lies in connecting the transformer secondaries in a manner that produces a harmonic-neutralized three-phase output voltage.

The transformer for each stage has three secondary windings with different turns ratios, chosen to provide a large amount of harmonic cancellation.[1] Each of these secondaries is connected in a different phase of the three-phase output—one in phase *A*, one in phase *B*, and one in phase *C*. The three sets of secondary windings produce a balanced three-phase output. Total three-phase capacity is approximately six times the kva rating of a single stage.

Output Wave Shape and Harmonic Distortion—Since any static inverter is basically a synchronous switch, the wave shape that is produced is a series of steps instead of a pure

[1] "Static Inverter with Neutralization of Harmonics," A. Kernick, J. L. Roof, T. M. Heinrich, *AIEE Transactions*, 61-891. 1962.

sine wave. The difference between such a stepped wave and a pure sine wave lies in the amount and kind of harmonic distortion that is present in the inverter output. A simple three-phase bridge inverter, for example, produces an output wave form containing harmonics totalling 40 to 50 percent distortion.

The Accur/Con inverter, because of its harmonic-neutralizing transformer connections, has a total distortion of approximately 15 percent with no filtering. More important, the first uncancelled harmonic is the eleventh, which is higher than most motor loads respond to. In fact, the only uncancelled harmonics (H) are those expressed by the simple formula:

$$H = 2kN \pm 1,$$

where N = number of stages and $k = 1, 2, 3 \ldots$

Thus, for a standard six-stage inverter, the only harmonics present are the 11th, 13th, 23rd, 25th, 35th, 37th, and so on.

The concern over harmonic distortion in wave shapes is far from academic. For one thing, harmonic distortion is useless energy and produces excessive motor heating. Also, motor stability problems are caused by harmonic distortion, especially by the lower harmonics. Filtering reduces distortion, but its effectiveness is limited in systems that must operate at different frequencies. Elimination of harmonics, as in the Accur/Con 200 system, strikes directly at the cause of the problem.

Continuity of Operation—Perhaps the most important single requirement of a power inverter for the continuous-process industries is continuity of operation. Loss of operation for only a few seconds can cause thousands of dollars loss in critical processes. For this reason, a component failure must not cause the inverter system to shut down.

Ordinary inverter systems are basically three-phase bridge inverters, arranged in different ways. In such inverters, failure of a single controlled rectifier, diode, or fuse instantly causes single-phasing and immediate shutdown under all normal load conditions.

The Accur/Con system is *not* basically a three-phase bridge inverter but rather a group of single-phase bridge inverters with transformer interconnection to produce a three-phase output. The significance of this, for reliability, is that loss of one controlled rectifier, diode, or fuse causes at worst the loss of one of the six stages. *It doesn't destroy the three-phase output*, but merely increases distortion and reduces the total system capacity. Therefore, the system can be shut down in an orderly manner or the load transferred to a spare inverter.

Servicing is simple, since indicating lights immediately tell which stage is in trouble. A straightforward checklist of go or no-go points can then be checked to locate the failed component.

Voltage Control—For successful adjustable-frequency motor operation, power must be supplied at essentially constant volts per cps. For example, a 220-volt 60-cps motor must be operated at 330 volts for 90-cps use, at 110 volts for 30-cps use, and so on. The same principle is true for transformers and other devices operating by magnetic induction.

Instead of speaking of volts per cps, the inverter designer speaks of volt-seconds per cycle, which is dimensionally the same. His reason is that volt-seconds are seen graphically as the area under the voltage wave. Supplying the motor requirements then is a matter of maintaining

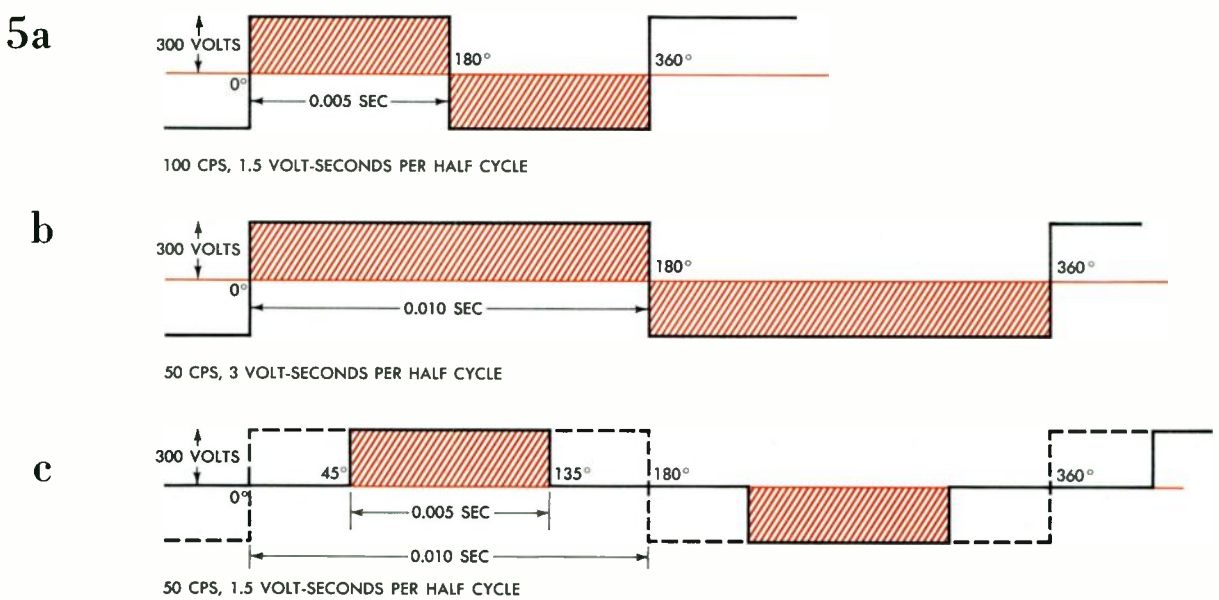

CONSTANT VOLT-SECONDS PER CYCLE are required by motors and other electromagnetic loads. This kind of output is achieved by pulse-width modulation. (*a*) In operation at 100 cps and 300 volts, for example, the magnetic flux in a half cycle is 300 volts × 0.005 second, or 1.5 volt-seconds. (*b*) If only the frequency were changed to 50 cps, the flux in a half cycle would be increased to 3 volt-seconds. (*c*) Reducing pulse width restricts the flux at 50 cps to 1.5 volt-seconds per half cycle. Pulse width is controlled by a logic circuit that automatically determines the proper pulse turn-on and turn-off times.

this area constant, regardless of the frequency of the inverter output.

For example, operation at 100 cps and 50 cps is shown in Fig. 5. The volt-second area of a half cycle at 100 cps is 1.5. If only the frequency were changed to 50 cps, the wave shape would be as shown in Fig. 5b, and the volt-second area would be 3. This would be totally unsatisfactory for magnetic devices. If, however, the wave form at 50 cps is made to look like that illustrated in Fig. 5c, then the volt-second area is again 1.5 as required.

Such a wave shape is achieved by delaying the output pulse turn-on and advancing the pulse turn-off, as directed by the logic signals. A simple but effective logic circuit makes this control an inherent characteristic of the inverter, greatly simplifying precise voltage regulation. The resulting pulse width is the same at all frequencies, assuring optimum performance of motors, transformers, and other devices supplied by the inverter.

Power and Frequency Ratings—Accur/Con 200 ratings presently range from 25 kva through 1000 kva. The 100-kva rating of the unit shown in the photograph is achieved with medium-power controlled rectifiers. Larger power ratings are produced by using more stages, by using a stage with larger controlled rectifiers, or both.

The addition of stages has several advantages. Total harmonic content is further reduced and the first uncancelled harmonic is made even higher. Perhaps more important, the stages are interchangeable, so a single spare stage can be used for several inverters.

The use of larger controlled rectifiers will require a different stage design because of thermal limitations. Presently, normal forced-air cooling over aluminum heat sinks is adequate. In the future, heat sinks for controlled rectifiers of higher power may be cooled by refrigerated air, water jacketing, or other methods.

The unit shown in the photograph has a frequency range of 90 to 15 cps. The range can be extended steplessly down to three cps, but with higher harmonic content. This is an extremely wide frequency range for inverters. Most other types are limited to ranges of about two to one, and switching of capacitors or transformers must be used to extend the range another two to one.

The wide range of stepless frequency adjustment has many process advantages. Machines that require threading can be run at very low speeds, for example, and then accelerated smoothly to normal production speed. Also, starting at low frequency permits use of an inverter sized strictly for running requirements. Inrush current due to linestarting of ac motors at running frequency would require a much larger inverter.

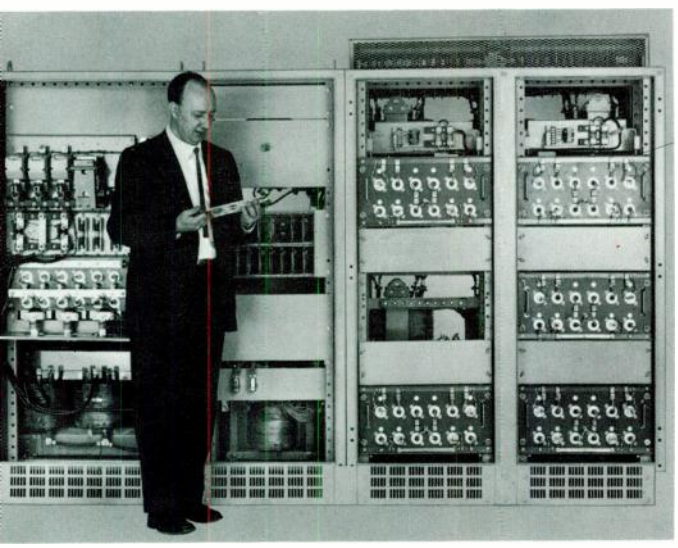

AN ACCUR/CON 200 power inverter with doors and safety covers removed. The left cabinet section houses the main dc power supply; the middle one, the master oscillator (*top*) and logic section (*center*). The double section at right contains the inverter stages, one of which has been removed. The unit shown here has a rating of 100 kva continuous, with peak capacity of 150 kva for 10 seconds. The peak rating is necessary for motor starting requirements.

Applications

Accur/Con inverter systems are by no means limited to precision speed-control applications in the man-made fiber industry. They are basically simple, static, highly reliable, highly efficient, and highly flexible adjustable-frequency systems, and they retain those characteristics regardless of their use.

A few of the other drive applications possible are for synchronized conveyors in assembly lines, automatic warehousing systems, and similar operations; runout tables in metalworking lines; plastic-film processing lines (casting, coating, stretching, and other operations); paper processing lines (coaters, slitters, smaller sectional machines, and other equipment); high-speed printing presses; and programmed acceleration and speed control for the electric powered vehicles that are used in modern rapid-transit systems.

Even though an adjustable-frequency system is more expensive than a single-motor adjustable-speed drive, inverters sometimes can be justified even for single motors. Nuclear power plants, for example, have canned-rotor pumps, with the drive motor located inside the coolant loop where water flows directly through the airgap. Since brushes, sliprings, and commutators are obviously unsuitable for this kind of service, adjustable-frequency power is used to control the motor speed. Simple squirrel-cage motors with adjustable-frequency control also solve hazardous-atmosphere problems, and they can operate at high speeds that would make brushes impractical for continuous service.

The first cost of inverters in systems requiring close speed control is competitive with that of rotating conversion equipment in most ratings. Installation cost is considerably less, as is the floor space requirement. Energy cost is substantially less because of the inverter's high conversion efficiency at all speeds and loads. Preventive maintenance consists only of such routines as cleaning air filters and checking fans, and simple trouble-shooting techniques make servicing fast and inexpensive. Investment in spare parts is less, both in money and in storage space. These advantages and the unmatched performance will bring static inverter systems into greatly increased use in industry.

The Lightning Prestrike Theory

S. B. Griscom, *Consulting Engineer, Electric Utility Engineering, Westinghouse Electric Corporation, East Pittsburgh, Pennsylvania.*

The prestrike theory, first introduced in 1958, proposes a mechanism that accounts for the behavior of the lightning stroke. However, field evidence is extremely difficult to obtain, and the disappointingly small amount of data gathered to date has not been sufficient to evaluate the theory. Results of laboratory tests by other investigators do tend to support the theory.

Electric power systems and equipment have a high degree of immunity to damage or service interruptions from lightning. This accomplishment is the result of continuing efforts in the collection of laboratory and field data and in theoretical analysis. But, in spite of this effort, some of the most fundamental aspects of lightning are still unexplained, or at least controversial. For example, while many theories have been advanced, the process by which clouds become thunderclouds is not yet established; or, after a cloud becomes a thundercloud, how a leader stroke is launched; or, after a leader stroke is launched, by what mechanism it advances toward earth.

The prestrike theory[1,2] to be described is concerned mostly with the last-named phenomenon and attempts to explain the step-by-step advance of the leader stroke.

Dielectric Strength of Air

A good starting point for studying lightning is the breakdown strength of air as obtained in laboratory tests, shown in Fig. 1. The curve covers a tremendous range and consequently omits details of some side effects. With uniform field electrodes (usually sphere gaps with a separation less than half their diameter), the dielectric strength of air varies from about 50 000 to 25 000 volts per cm over a 1-to-1000 variation in electrode separation. Thus, with uniform field electrodes, the dielectric strength of air is commonly taken to be about 30 000 volts per cm. Uniform field electrodes have shown little change in breakdown strength with the rate of rise of the test voltage.

With collinear-rod electrodes, dielectric strength varies from about 20 000 to 6000 volts per cm for gap-length ratios of 1 to 200, as also shown in Fig. 1. However, if the customary square-cut rod gaps were tested down to extremely small separations, they would probably show breakdown strengths of about those obtained with uniform field electrodes (as indicated by the dashed curve to the left of the full-line curve in Fig. 1).

Laboratory dielectric tests of air extend to gap lengths of only 15 to 20 feet, whereas lightning strokes span 10 000 feet and more, not counting the zig-zag and oblique paths. Cloud potentials are known to be in the range of 25 million to 150 million volts.[6] Therefore, if the same measure of air dielectric strength is used for lightning strokes as for laboratory tests (the *average* obtained by dividing voltage difference by gap length), an absurdly low value of 150 volts per cm is obtained. These circumstances—the difference between uniform field electrodes, collinear-rod electrodes, and cloud-to-ground discharges—suggest the possibility that the dielectric strength of air remains constant, but that different phenomena or regimes are encountered as gap width and length are changed. These regimes can be classified as follows:

Regime 1—Uniform field electrodes;
Regime 2—Nonuniform field electrodes with moderate spacings;
Regime 3—Nonuniform field electrodes with extra long spacings.

Actually, all of these regimes have been known for 30 years or more, but not so classified. For example, cloud-to-ground discharges are known to be a series of spark steps averaging about 70 feet in length (Schonland and others*),

**When a specific identification is not given here, the work is identified in references 1 or 2.*

1

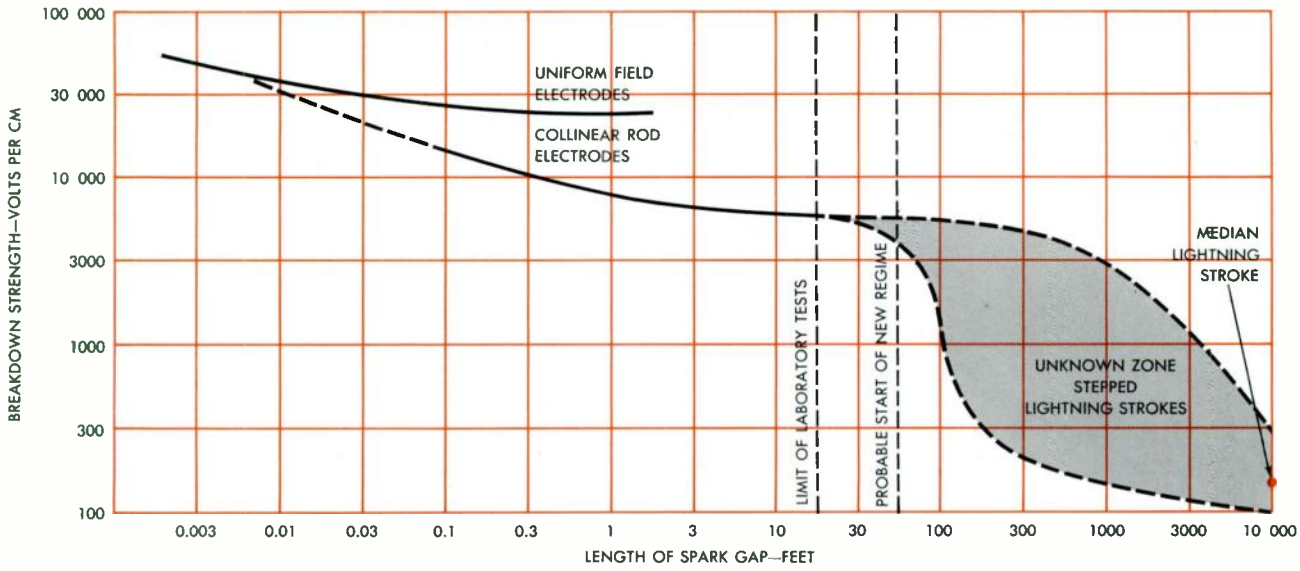

IMPULSE STRENGTH of air changes markedly for long spark gaps, suggesting a radical change in breakdown phenomena.

rather than a single continuous spark traversing the entire gap from cloud to ground.

Space Charge and Plasma Channels

Further discussion of the breakdown phenomena will require extensive use of two basic concepts—*space charge* and *plasma channel*.

Space Charge—True space charge is most properly defined as a gathering of electrons or protons in a vacuum. But as used here, the term means a predominance of negative or positive ions in air. In a typical electrified cloud cell, comparatively few molecules are charged despite the enormous total energy. Uncharged air molecules outnumber charged molecules by approximately ten million-billion to one. Borrowing an artifice often used by physicists, if one air molecule of a thundercloud is imagined to be the size of a marble, the next nearest molecule is about four inches away; but the distance between molecules bearing charges of like sign is about 12 miles! This large relative spacing of charged molecules probably explains why many electrified clouds do not cause lightning strokes; and why it is difficult to provoke lightning strokes from charged clouds by trailing grounded wires from balloons or rockets. Therefore, for present purposes, space charge is loosely defined as a volume of air space wherein a small fraction of the molecules are ionized at one dominant polarity. The dielectric strength of such an air volume on a uniform field basis is practically the same as ordinary air.

Plasma Channel—A plasma channel in air is well known to electrical engineers as a spark or arc. This channel of fairly good conductivity is made up of nonorbital electrons and positive nuclei. In this discussion, plasma channels result from intense local electric field gradients that forcibly detach electrons from their atomic nuclei and accelerate them to such high velocities that collisions with neutral atoms eject additional electrons, thereby elongating and heating the channel. Again, the definition is approximate, to shorten the description of complicated phenomena.

2

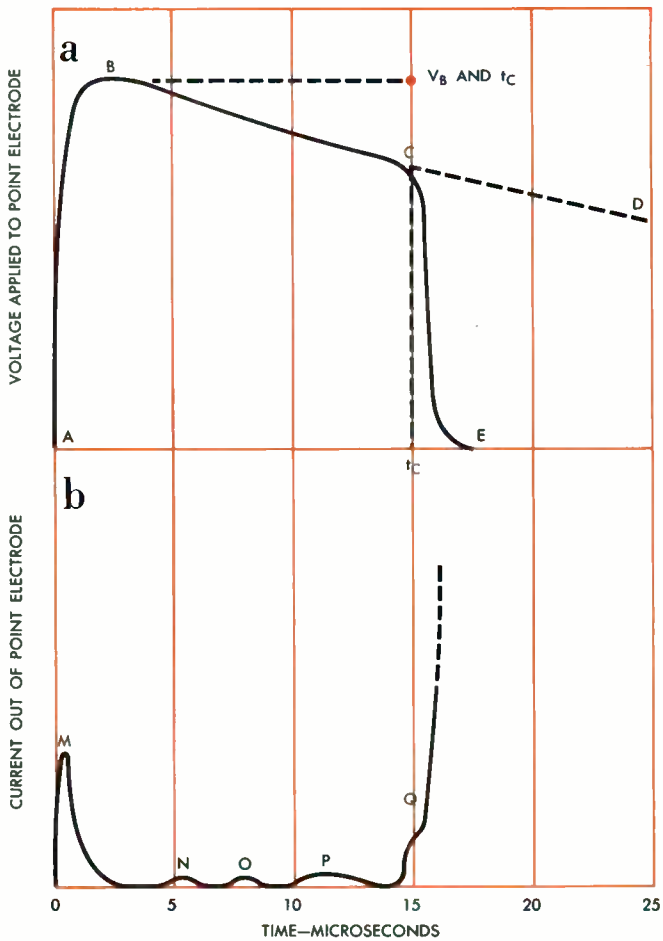

VOLTAGE-TIME CURVES (*a*) of applied voltage *ABCD* and for impulse flashover *ABCE* of a point-to-plane air gap. (*b*) Current-time curve *M* of current into the point electrode when no flashover occurs, or (to a different current scale) *MNOPQ* when a flashover occurs at time t_C.

Laboratory Data on Flashover

The impulse flashover characteristic of spark gaps or insulation is usually given by time-lag curves. An open-circuit impulse voltage shaped like *ABCD* (Fig. 2a) is produced by a surge generator and applied to a rod-to-plane gap. With large gap separations, a corona burst current will be drawn by the point electrode from the surge generator, whether the gap actually flashes over or not, provided the electric field intensity at the point electrode exceeds the 30 000-volts-per-cm dielectric strength of air. Special techniques are necessary to record this corona burst current, such as those of Park and Cones (1956), and Stekolnikov and Shkilev[3] (1962), since corona burst currents are weakly luminous and difficult to photograph.

A typical corona burst current pip is shown at *M*, Fig. 2b. These pips have sometimes been described as prebreakdown currents, or predischarge currents. However, gap breakdown is not a requisite for such current pips, which are principally due to the displacement or capacitive projection of charge into the gap space. The thermal or radiant energy component in a corona burst current pip is extremely small, as evidenced by the extreme difficulty in photographing them in the laboratory. A "predischarge current" cannot exist because current must be the result of charge movement. With special setups, corona bursts can be photographed, even when the applied voltage is less than 10 percent of that required for gap breakdown. The volume enclosed in the photographic envelope of the impulse corona burst contains space charge, and for impulse voltages well below flashover, the charge will drift slowly to the grounded plane.

Flashover conditions can also be described with Fig. 2. In a so-called "critical" flashover, the voltage wave will be as shown by *ABCE*. A corona burst occurs between *A* and *B* (Fig. 2a) and results in a much larger pip at *M* (Fig. 2b) than in the no-flashover case. True flashover starts at *C*, at a time t_C. Customary practice ignores the voltage at time t_C, and the flashover is designated by the crest voltage at *B*, a time-lag of t_C, and gap separation *s*. This procedure imputes a dielectric strength of V_B/s for air under the test conditions. While useful for engineering purposes, this procedure tends to give an erroneous concept of the physical nature of spark breakdown wherein, according to Fig. 1, the dielectric strength of air appears to vary from 50 000 to 150 volts per cm, with 6000 volts per cm—the *average* minimum strength in laboratory tests—seemingly of especial significance.

Further shown in Fig. 2b are current pips *N*, *O*, *P*, and finally an abrupt rise at *Q* to an eventual crest that is limited by the internal impedance of the surge generator. The process that occurs between time zero and time t_C is quite complicated. Park and Cones suggested an explanation that applies to part of the phenomena. The prestrike theory outlines a complete mechanism that applies to the long spark of lightning. Stekolnikov and Shkilev[3] have presented the best photographic and current-time data thus far available on long laboratory sparks, obtained by simultaneous use of an image intensifier and a synchronized optical shutter. They report a corona burst envelope radius of about 100 cm, with 1700 kv applied. This indicates an average gradient at the outermost parts of the corona envelope of 19 000 volts per cm. With this average gradient, the maximum gradient could well be 30 000 volts per cm or more. They also state, ". . . the negative (space) charge, carried by the impulse corona and the stepped leader into the gap, decreases the potential gradient in the vicinity of the high-voltage electrode and impedes the development of the leader from this electrode." This is one of the elements of the prestrike theory.

The Prestrike Theory

A pictograph of a lightning leader in one of its many pauses in its descent from a thundercloud to ground is shown in Fig. 3. If vastly reduced in size, Fig. 3 is the corona burst just discussed in connection with laboratory impulse tests of collinear-rod gaps or rod-to-plane gaps. The leader core is a plasma channel extending from the thundercloud to the leader core tip.

The condition represented by Fig. 3 is quasi-stable. The electric field intensity within most of the leader head is quite low by virtue of the integrated effect of the surrounding space charge. The leader core tip is an exception, because it and its forked branches have small radii of curvature. There will, therefore, be intermittent glow-type corona discharges from the branches of the leader core tip into the nearby space charge regions. These discharges are self-limiting, and the total current is small, being the corona loss current of the leader head as a whole. Any one leader core branch is of small diameter and rapidly cools and becomes nonconducting as it recedes toward the main leader core.

Instability of the leader head comes about from conditions on its irregular perimeter rather than near the leader core. The calculated vertical component of electric field for a smoothed outline of the leader head of Fig. 3 is shown in Fig. 5c. The average gradient for the smoothed outline is about 24 000 volts per cm, but gradients are much higher at protruding irregularities and much lower in the valleys between protuberances.

The stepping mechanism of the prestrike theory is illustrated in Fig. 4. Some details of the formation of the lightning leader head cannot be covered here. Skilling and Dykes, Park and Cones, and references 1 and 4 all present data or arguments indicating that impulsive charges can be projected into air space by a process that does not involve bright photographic tracks or bridging of a gap by channels of high conductivity. These references may be consulted for further information.

Only three protuberances are shown in the sequence of Fig. 4; an actual lightning leader head is three-dimensional, and many protuberances may progress simultaneously, but at varying rates. In Fig. 4, protuberance *O* was arbitrarily chosen to be the most active. The total time from Fig. 4a to 4e is about 50 microseconds according to Schonland and his associates. A rough timetable of the stages of Fig. 4 is given below:

Fig.	*Time (Microseconds)*
4a	0
4b	35
4c	45
4d	49
4e	50

At the instant illustrated by Fig. 4e, the highly conducting leader core plasma channel is suddenly connected to the

good conductivity plasma channel developing from the embryo leader head *O*. Previous to the junction of these two plasma channels, the amplitude of current in each is rather small; the junction results in a heavy pulse of current in both channels and produces a sudden enlargement of the new leader head of space charge at *O*. The current pulse is estimated to have an average crest value of 12 000 amperes. The pulse of current is drawn from the leader core previously established, but since it had cooled in the 49-microsecond time between Fig. 4a and 4d, a considerable amount of energy is required to re-establish good conductivity, and the dissipation of this energy results in a sudden, momentary increase in temperature of the channel. The channel extension to the new leader head (Fig. 4e) is

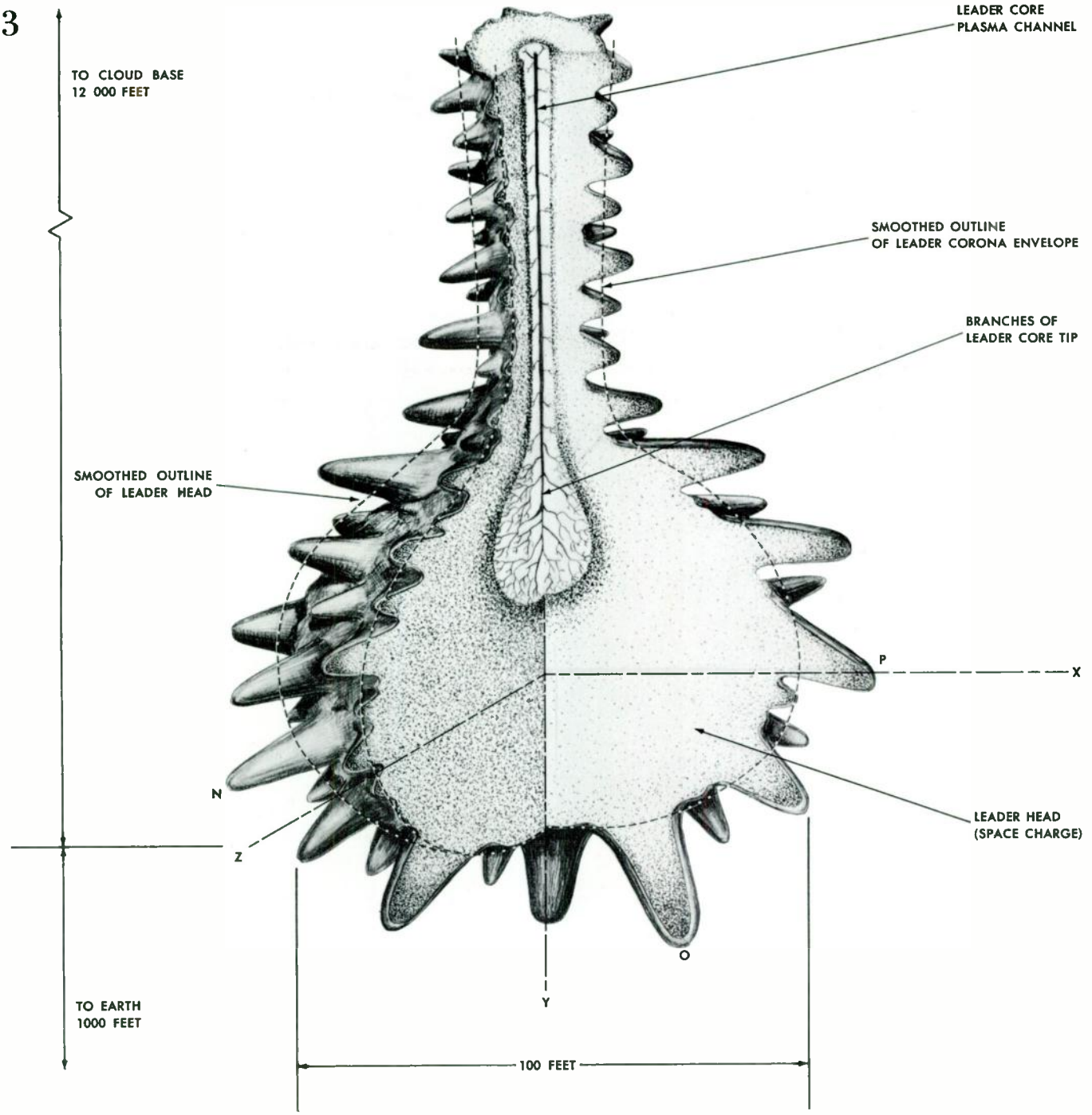

LIGHTNING LEADER AND LEADER HEAD according to prestrike theory are shown in this three-dimensional pictograph. The dots represent negatively charged air molecules and their spacing is an approximate indication of distribution of charge.

brilliantly luminous. The channel above the junction point is progressively re-illuminated at an appreciable fraction of the velocity of light. The zigs and zags of the path prior to Fig. 4a (see Fig. 5a) are reproduced as the pulse of current proceeds toward the cloud, progressively extracting charge from the established channel and the cloud to support each new extension.

Although the sequence shown in Fig. 4 primarily illustrates the step mechanism described in the prestrike theory, another effect is also accounted for—the branching or forking of lightning strokes. It is well known that except for strokes to high objects, lightning branches *always* diverge as earth is approached. Branching is readily explained by the stepping mechanism just described. Suppose that protuberances *N* and *P* in Fig. 4a were larger than *O*. Then plasma channels from those protuberances would reach the leader core without much mutual interference and would not need to do so simultaneously to produce a branching pair of new steps. Thus, the prestrike theory provides an explanation for this branching process, and also explains why branches are apt to make rather obtuse angles with each other.

The average concentration of charged molecules in the leader head is greater than in the thundercloud by perhaps 8000 times per unit volume. Even so, in the expanded scale described earlier, where a molecule is represented by a marble, molecules of like electric sign would be nearly a mile apart.

A system of plasma channels is shown withdrawing charge from the cloud in Fig. 5a. The average current flow is about 1000 amperes. The electric gradient within the leader, shown in Fig. 5c, is quite low except near the extremities. This is why the prestrike theory predicts that leader steps come by a process in which the breakdown of air in a leader head progresses from its periphery to the leader core, rather than from the leader core outward (as proposed in other theories). Direct photography of the natural lightning process has not yet been accomplished. However, the work of Stekolnikov and Shkilev[3] has shown this process to be true for long laboratory sparks. Their investigations have shown the formation of a corona burst at a pointed cathode, followed by a period in which there was virtually no luminosity and finally followed by a luminous positive charge from the plate electrode (anode), which traveled into the corona burst and eventually caused electrical breakdown.

Stekolnikov's tests show a mechanism similar to Fig. 4, although he used metallic electrodes and spark distances only 1/7 of the average step in natural lightning.

Field Testing a Theory

With a given physical theory, it should be possible to devise proof tests. But lightning stroke measurements are difficult because the stroke current or a replica thereof usually must be made to flow through the recording device. The average incidence of lightning is thought to be about 10 strokes per square mile per year. Therefore, a given instrument connected to a moderately high tower (say 100 feet) is extremely unlikely to get struck. Increasing tower height increases the probability of getting struck, but a higher tower is apt to change the character of the lightning stroke current.

One requirement in a lightning-recording instrument is the ability to record fast rates of change of current. Other requirements are low instrument cost, low installation cost, and reliability. A reasonable balance of these requirements has been obtained in the kine-klydonograph.[5] About 80 of these instruments have been installed on five electric power systems for several years. The rate of data collection has been disappointingly low, whether from an unusually low incidence of lightning, or otherwise. The data obtained is the joint property of all of the collaborating companies, and since a joint publication has not been made, detailed results cannot be given here. However, it can be stated that the lightning prestrike mechanism described has not been contradicted.

One of the characteristics of the lightning stroke described in reference 1 predicts a particularly high rate of rise of current during the first component of the stroke. The kine-klydonograph does not contain specific means to identify the sequence of the components, but if a sufficient number and variety of records are obtained, it is possible in some instances to deduce which component occurred first.

Cathode-ray oscillographs permit the time sequences of lightning stroke components to be determined, and attempts have been made to use them on transmission line towers for a good many years. So far as known, there have been no satisfactory CRO records obtained for strokes to low objects.

Installations of cathode-ray oscillographs to record strokes to tall objects have been made and operated intermittently during the last 25 years. They have important advantages compared with near-ground-level installations. They can yield as many as 50 stroke records per year. With a single installation, it is feasible to use refined instruments, and equipment can operate almost continuously.

Although much valuable information has been and is being collected by high-spire cathode-ray oscillograph installations, the applicability of this data to near-ground-level conditions must be considered carefully. One questionable aspect is the time to crest of the first stroke of a downwardly traveling leader. A high spire emits corona due to the thundercloud, and this emission may occur for several minutes prior to a stroke, and total a large fraction of a coulomb. When a leader stroke approaches the high-spire, the charge emission will be copious. Furthermore, in the few milliseconds before the stroke, the low mobility of the space charge will cause the spire to be closely surrounded by the space charge. Therefore, when the leader swerves toward the spire, it will first meet the space charge cloud around the recording tower. There will be a period during which the leader head space charge is neutralized or dissipated by the space charge around the high spire. This process is in space and results in a comparatively slow rate of rise of current in the high-spire tower as measured by the oscillograph.

A further effect that might cause a low rate of current buildup in an initial stroke is the time required to build up conductivity in the soil, if it should be dry or rocky, since this requires the progressive propagation of spark paths in the soil.

Neither of the above effects is present to significant degrees during subsequent discharges of multiple strokes, or for strokes to transmission lines of moderate height.

4

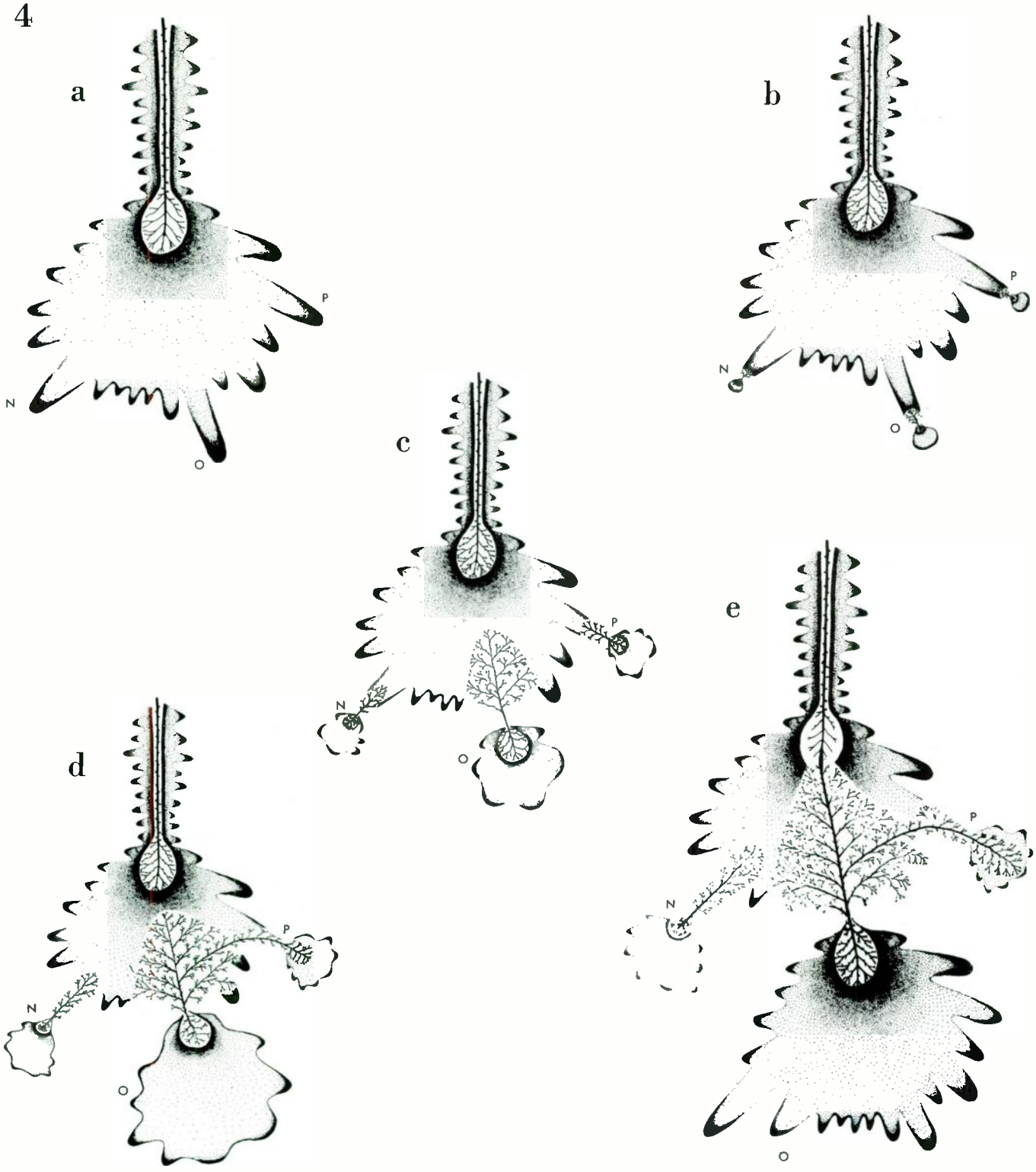

STEPPING MECHANISM by which the quasi-stable leader head gradually becomes unstable, and finally erupts and adds a new extension or step to the previous leader core:

(*a*) The leader head is in quasi-stable form, with extra long protuberances at *N*, *O*, and *P*. (*b*) These protuberances have become unstable due to ionization of air *outside* the protuberance and the withdrawal of charge from the protuberance, caused by plasma channels eating into the space charge and conductively carrying it into the three embryo leader heads. (*c*) Additional growth of the embryo leader heads. (*d*) A new situation is introduced when the plasma channels supplying the rapidly enlarging embryo leader *O* have merged with those previously feeding *P*; space charge is withdrawn from *P* and fed down into *O*. (e) The plasma channels feeding embryo leader head *O* have eaten their way to the leader core. This electrical junction is probably assisted by a sudden spurt of the original leader core toward the boring plasma channels from *O*. This process adds a brilliantly illuminated length of about 70 feet to the original leader from cloud to earth. The lowest part of (*e*) becomes stage (*a*) in the development of the next step.

Lightning Stroke Current

In this abbreviated description of the prestrike theory, the nature of the lightning leader stroke and the process accounting for the step-by-step progress of the leader from cloud to ground has been emphasized. The stepping mechanism accounts for the lightning spark across a very large air gap.

The lightning leader stroke removes electric charge from a diffusely charged cloud and deposits it around the leader core in the form of a corona envelope about 20 feet in diameter, but dependent upon the cloud potential. The process compresses the volumetric charge density by a ratio of about 50 000 to 1 compared to the density within the cloud. Consequently, when the leader head and then the leader core strike earth, or a transmission line, large currents can flow. The path of the leader stroke, with all its zigs and zags and branches is re-illuminated with great brilliance, the effect starting at the struck point and traveling upward toward the cloud.

From Schonland's work, the column of intense luminosity and the neutralizing electric charge, called the *return stroke*, is known to move upward at a velocity of about 0.3 to 0.1 the velocity of light.

With this knowledge and deducible information on the amount of space charge around the leader core, stroke current can be calculated. For example, if a leader has a charge of 200 microcoulombs per foot and a charge collection rate of 0.2 the velocity of light (0.2×984 feet per microsecond), the current will be:

$$I = \Delta Q/\Delta t$$
$$= \frac{200\times10^{-6}\times0.2\times984}{10^{-6}}$$
$$= 39\ 000 \text{ amperes}$$

This particular value of current is somewhat above the median value of lightning current as obtained by magnetic link recorders, although there is some suspicion that these statistics may be "loaded" with low-current readings resulting from power-frequency fault currents rather than lightning stroke currents.

Since the leader head is first to contact earth, and since it carries a much greater charge per unit of length than the leader, the prestrike theory concludes that a "spike" of current will precede the principal return stroke current just calculated.

A New Theory

Natural lightning has been studied continuously since the days of Benjamin Franklin. In this time, more than a dozen theories have been proposed to explain its mechanisms, most of which have since been disproved by experiments or counter arguments.

At present, the prestrike theory is the only theory that satisfactorily explains: 1) The zig-zag steps of the stroke path; 2) the uniform pause of 50 microseconds between each step in the leader stroke; 3) the average length of 70 feet for each zig-zag step; 4) the process by which branching or forking takes place; 5) the obtuse angles between steps and between branches and the main stroke path; and 6) a correlation between Boys camera photographs and the electrical processes of the stroke. The prestrike theory also accounts for certain time-lag phenomena that occur during the breakdown of air gaps subjected to impulse voltages.

The prestrike theory described here in a simplified manner is not yet established, but field testing is in progress toward that end.

5

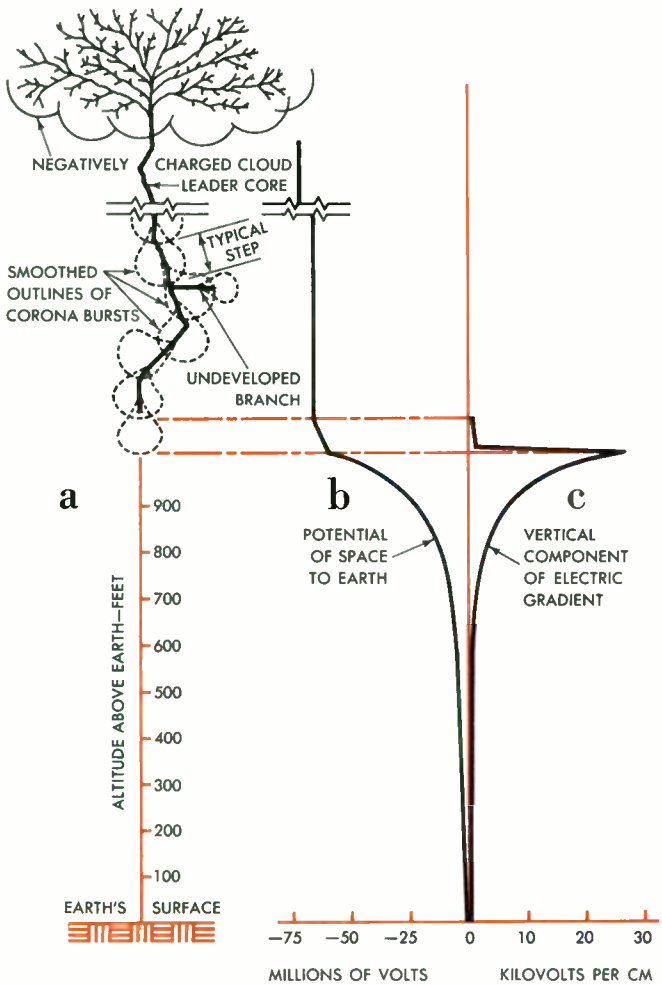

LEADER STROKE (*a*) progresses step-by-step earthward from thundercloud. Air space potential (*b*) calculated for a typical leader head poised 1000 feet above earth. Vertical component of electric gradient (*c*) calculated for this same leader head. Note that the gradient is greatest external to the head and least near the tip of the leader core.

References

[1] "The Prestrike Theory and Other Effects in the Lightning Strokes," S. B. Griscom, *AIEE Trans.*, vol. 77, pt. III, 1958.

[2] "The Influence of the Prestrike on Transmission-Line Lightning Performance," S. B. Griscom, J. W. Skooglund, A. R. Hileman, *AIEE Trans.*, vol. 77, pt. III, 1958.

[3] *New Data Regarding the Development of a Negative Spark and Its Comparison with Lightning*, I. S. Stekolnikov and A. V. Shkilev, Reports of the Academy of Sciences of USSR, 1962, vol. 145, no. 4—Physics.

[4] "Impulse Corona and the Prebreakdown Mechanism of Long Sparks," J. J. Kritzinger, *Nature*, March 23, 1963.

[5] "The Kine-Klydonograph—A Transient Wave Form Recorder," S. B. Griscom, *AIEE Trans.*, vol. 79, pt. III, 1960.

[6] "The Initiation of Long Electrical Discharges," C. E. R. Bruce, *Proc. Royal Society*, A, vol. 183, 1944.

Improvements in Photovoltaic Energy Converters

K. S. Tarneja, *Senior Engineer, and* R. K. Riel, *Manager, Special Products Engineering Department, Semiconductor Division, Westinghouse Electric Corporation, Youngwood, Pennsylvania.*

Solar cells are practical devices for converting radiant energy from the sun into useful electrical energy, and constant improvement is making these photovoltaic energy converters more efficient and more reliable. One major development is the large-area solar cell made from silicon sheet material.

Photovoltaic energy converters, commonly called solar cells, have been applied in terrestrial devices for many years. More recently, they have come to be used in large numbers as power supplies in earth satellites and other space vehicles; in fact, almost everything that is shot into space presently has its electric power supplied by solar cell panels. This is because the sun's energy is free in outer space and, at present, the solar cell is the most efficient device for converting this free solar radiation to useful electric power.

The importance of efficient and reliable power supplies in outer-space applications has added considerable impetus to the development work being done on solar cells. The main objectives have been improvement of the cells' power output, protection against radiation damage, and cost reduction.

Most of the development effort in this country has been in fabrication and design improvements in silicon semiconductor solar cells. The reasons are that the semiconductor devices are more highly developed than other types of photovoltaic energy converters, growth and fabrication techniques are more advanced with silicon than with some other semiconductor materials, and silicon is less expensive than other semiconductor materials. Other approaches are being investigated, however, including new materials such as gallium arsenide and new designs such as large-area thin-film cells. Perhaps the most advanced program is the development by Westinghouse of large-area solar cells on silicon sheet material.* This approach will be described after a brief explanation of what semiconductor solar cells are and how they work.

The authors wish to acknowledge the work of H. A. Wehrli and S. N. Dermatis in growing silicon sheet material for the large-area solar cells described in this article, of M. S. Shaikh and V. A. Rossi in fabricating the cells, of R. D. Lamb in making the efficiency measurements, and of P. F. Pittman for solar-cell application studies. Much of the work described here was supported by the U. S. Air Force Aeronautical Systems Division, Wright-Patterson Air Force Base, Dayton, Ohio.

Solar Cell Principles

Silicon is located in group IV of the periodic table of the elements; in a theoretically perfect crystal, each atom's four valence electrons form covalent bonds with four neighboring atoms. That is, the two electrons in each bond are shared equally by two atoms. However, heat, light, or an applied electric field can excite an electron from the valence energy band to the conduction band, thus breaking a covalent bond. This removal of an electron from its normal place in the crystal structure simultaneously leaves an empty place, called a hole, in the structure. The process is known as pair production, the "pair" being an electron and a hole.

The electron is free to move about in the crystal. The hole, too, can be thought of as free to move, since an electron from an adjacent bond can move into it and thus in effect cause the hole to move to the location formerly occupied by that electron. Since the atom that gave up the electron now has a net positive charge, the hole itself can be thought of as a positive charge moving about in the silicon crystal.

The single-crystal silicon used in semiconductor devices is either N type or P type. It is made so by "doping"—introducing into the crystal a very small amount of another element. N-type material is formed by doping with elements from group V of the periodic table, such as phosphorus. The atoms of these elements have five valence electrons. Since only four valence electrons are needed for the bonds with silicon atoms, one electron of each phosphorus atom in the crystal is free to move about. N-type material thus has an excess of electrons in its crystal structure.

P-type silicon is made by introducing an element from group III of the periodic table, such as boron. The atoms

of these elements have only three valence electrons, so each one can bond itself to only three silicon atoms by sharing electrons. The result is a deficiency of one electron (a hole) in a bond between the boron atom and an adjacent silicon atom. P-type material thus has an excess of holes.

In N-type material, the free electrons (most of them produced by doping, a few by pair production) greatly outnumber the holes (produced by pair production). Therefore, the electrons are called majority carriers and the holes minority carriers. In P-type material, the situation is reversed.

The basis of the semiconductor solar cell is the P-N junction, a region in a single crystal of semiconductor material at which a P-type layer and an N-type layer come together. The starting material is a crystal wafer that was doped while it was being grown to make it either P or N type. One face of this wafer is exposed to a vaporized dopant of the opposite type, which diffuses into the silicon to a depth of about half a micron and in sufficient quantity to overpower the original doping and change the material to the opposite type. The result is a piece of silicon with a P-N or N-P junction about half a micron below the surface of one face.

A cell made by diffusing a P-type dopant into an N-type silicon wafer is sketched in Fig. 1a. (This is the configuration assumed in the discussion that follows.) A soldered contact at the wafer's base forms the negative contact, and a grid structure soldered to the top surface is the positive contact.

The action of this cell when exposed to light is diagrammed in Fig. 1b. Light falling on the surface is absorbed rapidly as it penetrates the silicon. Part of this absorbed radiant energy disrupts covalent atomic bonds in the crystal, producing electrons and holes in pairs. For silicon cells, this requires an energy of about 1.12 electron volts, which excludes the usefulness of any radiation of wave lengths longer than 1.2 microns.

The minority carriers of the hole-electron pairs wander about in the region of their generation until they either recombine with majority carriers or cross the junction. The only useful carriers are those that go across the junction. They cause the crystal to become biased, with the P-type region positive and the N-type region negative. The bias causes a useful current to flow when the two regions are connected by a conductor. It also biases the junction in the forward direction so that it carries current.

The conversion efficiency (η) of a solar cell is represented by the relationship:

$$\eta = \frac{P_{max}}{A \times N}$$

where P_{max} = maximum power delivered by the cell, in milliwatts,

A = cell area, in square centimeters, and

N = solar energy density incident per second, expressed as number of suns.

(On earth one "sun" is light intensity equal to 100 milliwatts per square centimeter, while in outer space it is about 140 milliwatts per square centimeter.) Theoretically, a silicon solar cell should have a conversion efficiency of about 21 percent, but a number of practical limitations reduce the actual efficiency.[1] The main limita-

Solar Cell Relationships

The solar cell circuit is represented schematically in the figure. I_G is generated current, I_F is current flow through the junction, R_{SH} is shunt resistance (the internal resistance of the N-type layer), I_{SH} is current flow in the shunt resistance, R_{SER} is series resistance (the internal resistance of the P-type layer), R_L is load resistance, and I is current flow through the load.

The basic relationships that can be manipulated in solar-cell design are represented by the following equations:

$$I = I_G - I_O \left[\exp \beta(V + IR_{SH}) - 1\right] - V + IR_{SER}/R_{SH}$$

$$V_{OC} = 1/\beta \ln I_G/I_O$$

$$V_B = KT/Q \ln P_P/P_N$$

$$I_{SC} = I_G (1 - R_{SER}/R_{SH})$$

$$I_O = [QP_N (D_P/\tau_P)^{\frac{1}{2}} + QN_P(D_N/\tau_N)^{\frac{1}{2}}] \times \text{area},$$

where V_{OC} = open-circuit voltage

$\beta = Q/AKT$

I_G = generated current

I_O = reverse saturation current

V = voltage developed across the load

V_B = built-in voltage

I_{SC} = short-circuit current

P_N, P_P = equilibrium density of holes in the N region and the P region

N_P = equilibrium density of electrons in the P region

D_P, τ_P = diffusion constant and lifetime of holes in the N region

D_N, τ_N = diffusion constant and lifetime of electrons in the P region

R_{SER} = series resistance

R_{SH} = effective shunt resistance.

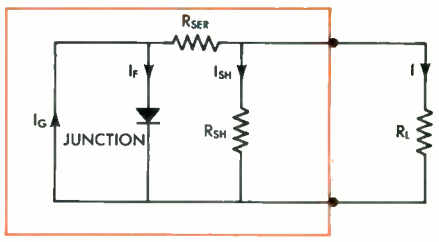

tions on the efficiency of the solar cell are reflection losses, incomplete collection of the pairs of holes and electrons, and series resistance losses.

Development

Much development effort has been aimed at finding ways of collecting as many of the generated pairs as possible by increasing the probability that they will diffuse across the junction. One way of doing this is by chemical surface treatment to remove surface damage caused by cutting and lapping. Such damage tends to trap the minority carriers, increasing the probability of their recombination. Another way is by making the diffused layer shallow so that minority carriers generated in it do not have to travel far to cross the junction.

The equations in *Solar Cell Relationships*, p. 180, suggest other measures that can be taken to maximize conversion efficiency. For one thing, use of high-lifetime material results in high current production. ("Lifetime" is the average time interval between generation and recombination of minority carriers; the longer it is, the better are the chances of minority carriers surviving long enough to cross the junction.) Lifetime is an inherent quality of a semiconductor material. It varies directly with the material's resistivity, so experimentation is employed to find optimum compromises between high lifetime and low resistivity.

Open-circuit voltage can be maximized by increasing the built-in potential; that is, both sides of the cell should be heavily doped.

Series resistance, which is the internal resistance of the diffused layer in the cell, is reduced by using a diffusion process that produces a high concentration of carriers at

1a

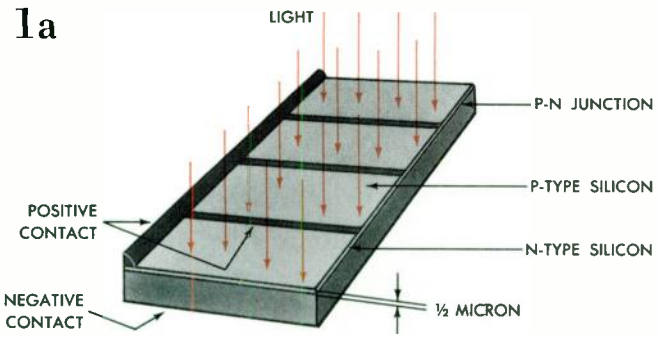

b

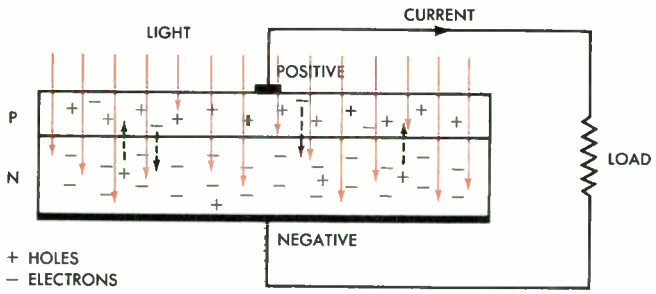

A SEMICONDUCTOR SOLAR CELL consists essentially of a thin wafer of single-crystal semiconductor material with contacts at top and bottom. (*a*) In this example, the silicon base material is of N type, and a thin top layer of P type has been formed by diffusion. (*b*) Light disrupts atomic bonds in the solar cell crystal to form pairs of holes and electrons. Some of the holes in the N-type region and electrons in the P-type region move across the junction. This creates a bias in the crystal that produces a useful external current when the two regions are connected by a conductor.

2a

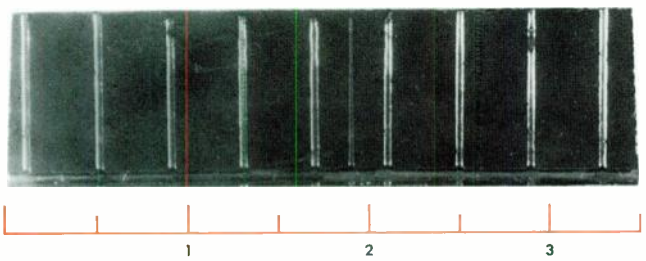

b

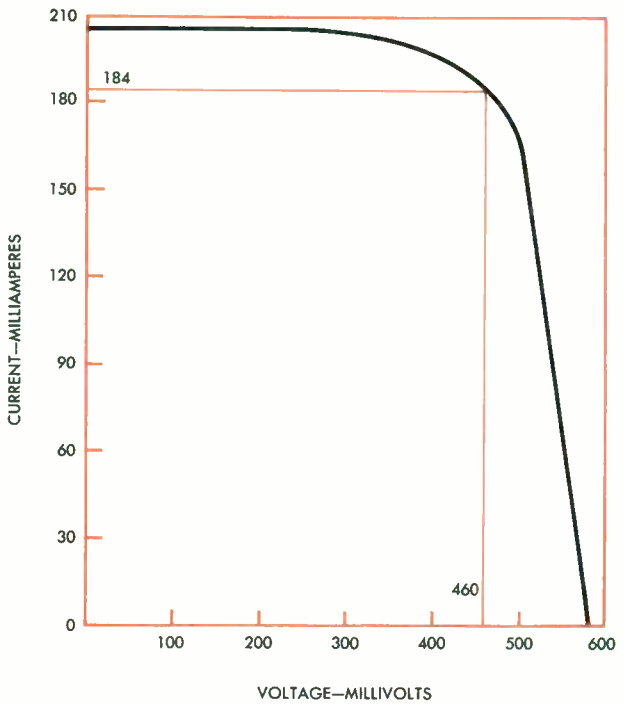

THE FIRST SILICON-SHEET SOLAR CELLS (*a*) were produced on short lengths of the material. (*b*) Typical voltage-current characteristics of one such cell. The intensity of the tungsten light source used for the measurements was 80 milliwatts per sq cm (0.8 sun). The largest rectangle that can be inscribed under the curve determines the maximum power delivered by the cell (85 milliwatts, for this one). With an active area of 8.2 sq cm, the cell's conversion efficiency is 13 percent. This efficiency is comparable to that of conventional cells.

the surface of the material. It is also reduced by using grid contacts instead of point contacts for the surface terminals. Grid contacts consist of a metal bus bar and grid soldered to the top surface of the cell, as shown in Fig. 1. The grids reduce the distance that minority carriers have to travel in the top layer to get to the contact. This offsets the resistance-increasing effect of making the top layer very shallow, a measure that we have seen is taken to maximize the probability of minority carriers in the top layer diffusing across the junction.

Additional improvement has been made in the silicon solar cell by improving its spectral response to sunlight. When a cell is placed in sunlight with the P-type layer exposed, the output current comes from electrons and holes generated within a diffusion length on both sides of the junction. ("Diffusion length" is the average distance minority carriers diffuse between generation and recombination.) The long wave lengths of light penetrate more deeply than do the short wave lengths. Consequently, the long-wave-length part of the spectral response is due to diffusion of holes in the N-type base material to the junction, where they are collected. The short-wave-length part of the spectral response is due to collection of electrons from the P-type region.

Unfortunately, the high temperature of the diffusion process used to form the junction produces imperfections in the crystal lattice and thereby lowers the lifetimes of minority carriers in the P-type region. This reduces the probability of carriers from that region reaching the junction. However, present-day techniques allow such close control of diffusion that an extremely shallow diffusion depth can be obtained—about half a micron. This allows more carriers generated in the P-type region to reach the junction, so the contribution from light in the short-wave-length part of the spectrum is greater. This approach has to be coupled with grid contacting and removal of the surface defects.

Solar cells used in outer space are subjected to radiation, which is most intense in the Van Allen belt and during solar flares. The Van Allen belt consists of both protons and electrons, while solar flares produce fluxes of protons predominantly. Both types of radiation inflict damage that

3a

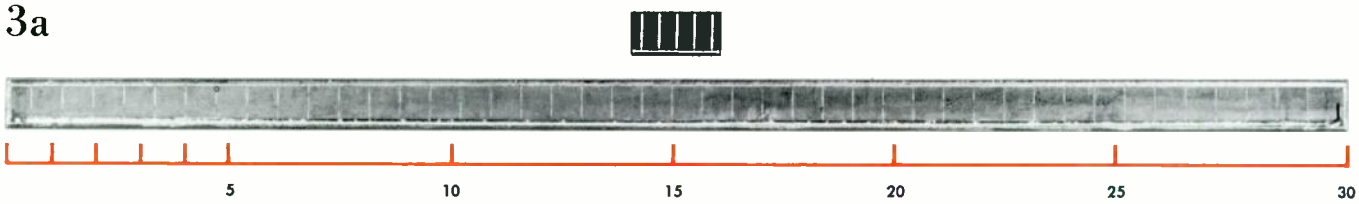

b

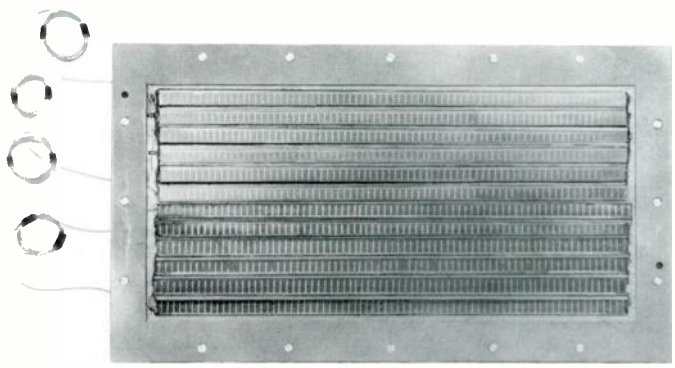

THE GREAT INCREASE IN AREA gained by using silicon sheet material (*a*) is illustrated by comparing one of the new cells (bottom) with a conventional cell (top). The former measures 1 by 30 by 0.05 cm, while the latter measures only 1 by 2 by 0.05 cm. This large area reduces material waste in cell fabrication and also reduces the number of fabrication processes required. (*b*) This experimental solar-cell panel is made from 12 large-area cells, each measuring 1 by 30 by 0.05 cm. Use of large-area cells requires far fewer connections than would be needed in a panel made up of the conventional small cells. This improves reliability and reduces weight and volume.

4

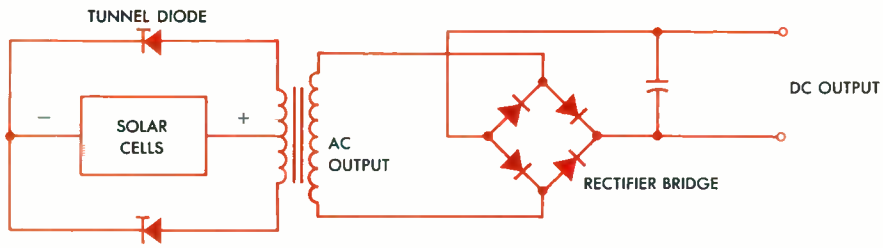

RAISING OUTPUT VOLTAGE of solar cells to a higher level can be accomplished with static circuits such as this. The primary side of the transformer contains tunnel diodes and an array of solar cells. The circuit constants are so chosen as to cause the tunnel diodes to key on and off in a push-pull, out-of-phase sequence that drives the transformer primary winding. The ac output of the secondary winding can be rectified by a full-wave bridge, if desired, to change it back to dc power.

reduces conversion efficiency. The basic effect of radiation damage is a decrease in a cell's short-circuit current (current obtainable with zero load) caused by reduction of the lifetime in the base region.[2]

Radiation damage has been reduced by applying quartz windows and organic films that shield the cells against radiation. Also, solar cells fabricated by diffusing phosphorus into P-type silicon are more resistant to radiation damage than the conventional P-N type.[3]

Thus, intensive research and development efforts have greatly improved the silicon solar cell. Evaluations in test facilities that simulate outer space show that cells of the present design have a maximum conversion efficiency of about 13 percent in outer space. Further efforts to increase efficiency, reliability, and radiation resistance and to reduce cost are in progress at several locations. The immediate approach at Westinghouse to fulfill present requirements, reduce cost, and improve reliability is to use silicon sheet material.[4,5,6]

Silicon-Sheet Solar Cells

The standard procedure in making silicon solar cells has been to grow silicon single crystals about an inch in diameter and then slice these bars into wafers 0.025 inch thick. The wafers are diced into 1- by 2-cm blanks, which are lapped to remove surface damage, cleaned, and etched. The wafers are then diffused, contacts are applied, and the cells are tested.

Silicon sheet material, on the other hand, is grown from the melt as a single-crystal ribbon of the desired thickness. Sawing, dicing, and lapping are not required, so the number of fabricating operations needed to produce a given light-collecting area is greatly reduced. So is the amount of material waste. Because the cells are much larger in area than the conventional cells, far fewer connections are required to produce a panel with a given power output; this improves the panel's reliability and reduces its weight and volume.

Silicon sheet is material that has solidified, under controlled conditions, between dendrites (long narrow crystals). The key to sheet growth is a proper seed crystal. This seed is inserted into the melt and a button allowed to form on it. Two "wings" form on the button, and pulling is then started. A dendrite grows on each wing, with the space between the dendrites filled by silicon sheet. The degree of supercooling and the pulling rate control the thickness of the material. The dendrites on the edges control the width and also support the sheet.[5]

The length of the sheet that can be grown is limited only by practical considerations such as available work space. The sheet can be wound on a reel as it is formed, if desired. The dendrites are removed from the two edges of the sheet, and the material is then ready for fabrication of solar cells.

Most present silicon-sheet solar cells are of the P-on-N variety made by diffusing boron into N-type material. Phosphorus diffusion into P-type material is also used.

The first cells made from sheet material were prepared on small lengths of the sheet (Fig. 2). Typical conversion efficiency was 13 percent. This is comparable to the efficiency of conventional cells as determined by laboratory measurements with a standard tungsten light source.[7]

The principal improvement achieved with this development is, of course, the tremendous increase in the area of the cell. It is difficult to fully appreciate this improvement until the two types are compared directly as in Fig. 3a. The conventional cell's active area is 1.8 sq cm, while the silicon-sheet cell in this photograph has an active area of 25 sq cm. (The active area of a cell is somewhat smaller than the actual area because the grid and bus bar cover part of the surface.)

Conversion efficiency of the large-area cells is now nine percent. Much higher efficiencies can be expected because the cells' open-circuit voltage is good (580 millivolts) and their current output should be increased considerably by improvements in diffusing and processing techniques. Also, processing and fabricating costs should decrease as manufacturing techniques are refined.

Experimental power-producing panels have been made by assembling a number of the large-area silicon-sheet solar cells (Fig. 3b).

Applications

Semiconductor solar cells are used in large numbers to provide power in outer space. The cells are inherently low-voltage devices, so for space (and many terrestrial) applications the first step in using their power output is raising the voltage. The only known approach is to convert the dc output to ac power and raise the voltage with a transformer. The power can then be rectified back to dc power, if desired.

One way of accomplishing this energy conversion is diagrammed in Fig. 4. With inputs of 150 to 170 millivolts, this circuit has produced an output of 20 volts peak to zero, or 40 volts peak to peak.

On earth, solar cells serve such uses as powering remote telephone lines, police call boxes along the highways, radio transmitters, and electronic navigation beacons. They have also been used to power transistor radios and electric clocks and as photocells for various types of instrumentation. The cells can be used as the sensing elements of tachometers, and they are also useful as temperature sensors because their power output decreases as temperature increases. Many other uses will be economically feasible as continued development and volume production decrease the cost of the cells.

References

[1] "Limitations and Possibilities for Improvement of Photovoltaic Solar Energy Converters," M. Wolfe, *Proceedings of the IRE*, July 1960, p. 1247.

[2] "Electron Voltaic Study of Electron Bombardment Damage and Its Threshold in Germanium and Silicon," J. J. Loferski and P. Rappaport, *Physical Review*, Vol. 98, April–June 1955, p. 1861.

[3] "Comparison of P-N and N-P Silicon Solar Cells," J. Mandelkorn, J. Kesperis, C. McAfee, W. Phoro, and D. Schwartz, *Proceedings of the Fourteenth Annual Power Sources Conference*, May 17–19, 1960, p. 42.

[4] "Silicon Dendrite Studies," S. N. Dermatis and J. W. Faust, Jr., *Journal of the Electrochemical Society*, vol. 107, August 1960, p. 188C.

[5] "Silicon Sheets for the Manufacture of Semiconductor Devices," S. N. Dermatis and J. W. Faust, Jr., CP-62-514, AIEE Winter Meeting, January 1962.

[6] "High-Efficiency Solar Energy Conversion," R. K. Riel, J. P. McKelvey, K. S. Tarneja, and M. S. Shaikh, Northeast Electronics Research and Engineering Meeting (NEREM), November 1960.

[7] "An Investigation of Solar Capabilities for Satellite Application," R. W. Runnels, *ASD Technical Report 61-334*, Armed Services Technical Information Agency (ASTIA), Arlington Hall Station, Arlington 12, Va.

96-Kmc Millimeter Wave Maser

An operating 96-kilomegacycle (10^9) millimeter wave maser with a pump frequency of only 65 kmc was first demonstrated in December 1961 at the Westinghouse Air Arm Division.

The unit was built under contract to the Thermionics Branch of the Air Force's Electronic Technology Laboratory, Aeronautical Systems Division, Wright-Patterson Air Force Base. This maser development is part of an investigation by the Thermionics Branch into the feasibility and power limitations of high-frequency coherent microwave amplifiers. This was the first time that microwave amplification by maser principles had been achieved at this high a microwave frequency, and also the first time that low-frequency pumping had been achieved with so large a ratio between signal and pump.

Pumping Frequency

A fundamental limitation of the conventional three-level maser is the need for pumping power at a frequency that must exceed the operating frequency. The reason for this can be shown by a brief review of maser operation.

By the rules of quantum theory, atoms can have only certain definite paramagnetic-spin energy levels, as determined by the spin configurations of the electrons in the shell of the atom. Therefore, an atom can change energy levels only by emitting or absorbing energy in quantum amounts,

$$E_2 - E_1 = h\nu$$

where E_2 and E_1 are permitted energy levels, ν is frequency of the applied electromagnetic field, and h is *Planck's constant*.

A typical three-level maser employs active atoms with three energy levels, as shown in Fig. 1. Normally, most of the atoms will be in the lowest energy (ground) state. To achieve *population inversion*, necessary for maser operation, atoms must be "pumped" to a higher (excited) energy state by applying an electromagnetic field of frequency:

$$\nu_p = (E_3 - E_1)/h,$$

1a

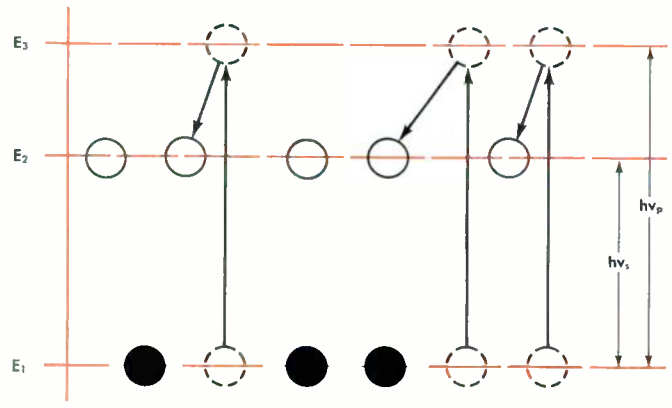

b

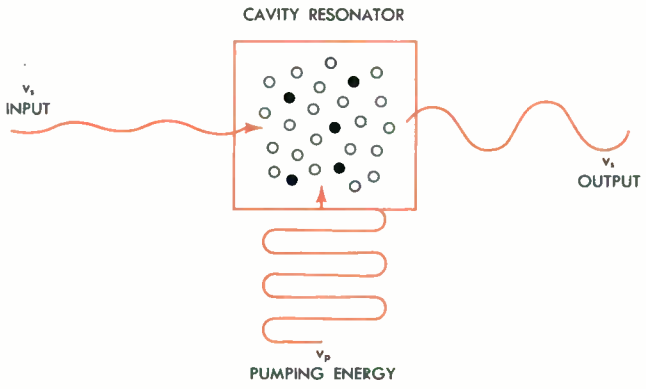

THREE-LEVEL MASER uses active atoms at three energy levels. Energy level diagram is shown in (*a*). Pumping energy at frequency ν_p is applied to produce population inversion in cavity (*b*), so that input signal at frequency ν_s is amplified.

SPACED-COIL SOLENOID is 3.75 inches long, has a 2.5-inch inside diameter and a 4.5-inch outside diameter. The iron-doped rutile maser with its orienting mechanism can be seen inside the superconducting solenoid.

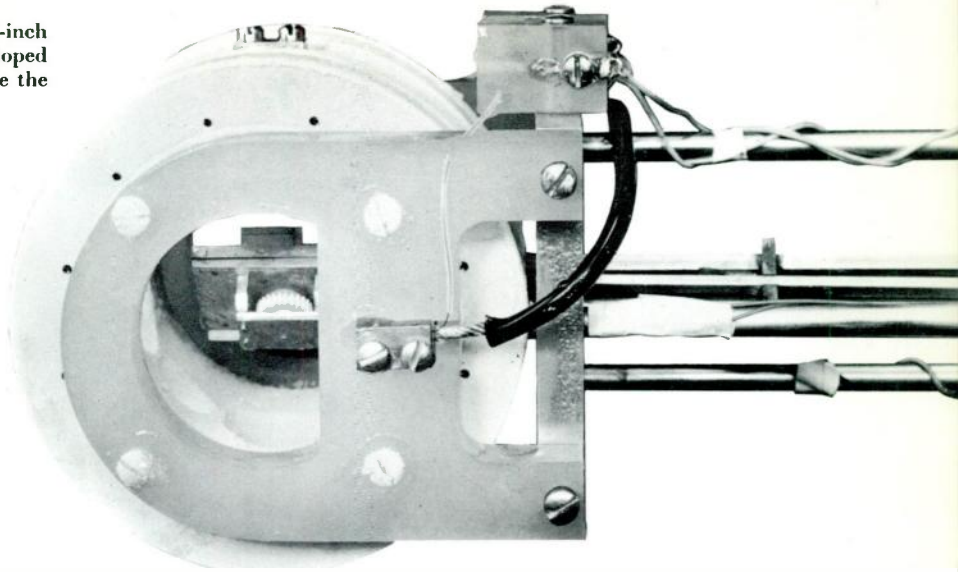

where v_p is the pumping frequency. The atoms fall back to a lower energy level, E_2, giving up excess energy, usually in the form of heat. If pumping is sufficient to produce population inversion of level E_2 over E_1, an electromagnetic signal field of the proper frequency,

$$v_s = (E_2 - E_1)/h,$$

will cause more atoms to release energy than to absorb energy, and the signal field is amplified (hence the name MASER—*M*icrowave *A*mplification by *S*timulated *E*mission of *R*adiation). Since $(E_3 - E_1)$ is always greater than $(E_2 - E_1)$, pumping frequency v_p must always be higher than signal frequency v_s. Therefore, the maximum operating frequency of such an amplifier is limited by the availability of high-frequency microwave oscillators.

The first specific proposal for a method of pumping at lower frequency than the signal frequency was made by the Westinghouse Research Laboratories; this instigated further development work at the Air Arm Division, and resulted in the 96-kmc maser, developed by W. E. Hughes.

In this new maser, five paramagnetic-spin energy levels are employed to obtain inversion. Pump frequency is considerably lower than signal frequency, so that the operating frequency is no longer so restricted by pump source availability.

Operation of the five-level maser is demonstrated in Fig. 2. Atoms are pumped from the lowest to the highest energy level in two equal steps, E_1 to E_3, and E_3 to E_5. Since these are equal-energy transitions, pumping can be accomplished with a single pumping frequency. To assist in obtaining the desired population inversion of E_5 over E_2, atoms are also pumped from E_2 to E_4, a transition which is again made equal to the other pumping transitions so that the same pumping frequency can be used. If signal energy is now applied

$$v_s = (E_5 - E_2)/h,$$

amplification can be obtained for a signal frequency higher than pumping frequency.

Obviously, the key to successful operation of such a

2

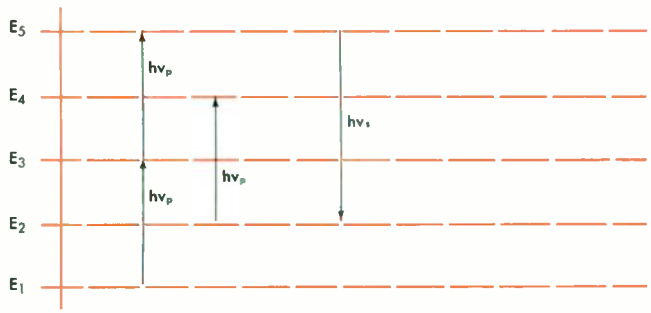

FIVE-LEVEL MASER has energy levels arranged so that pumping frequency v_p produces a population inversion of E_5 over E_2.

ENERGY LEVELS of Fe^{3+} in TiO_2 are a function of magnetic field. The crystal is positioned so that it is on a paramagnetic resonance at both signal and pump frequencies.[1]

3

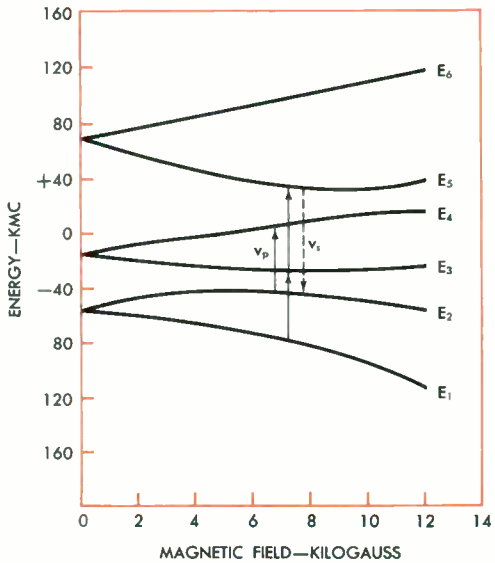

4

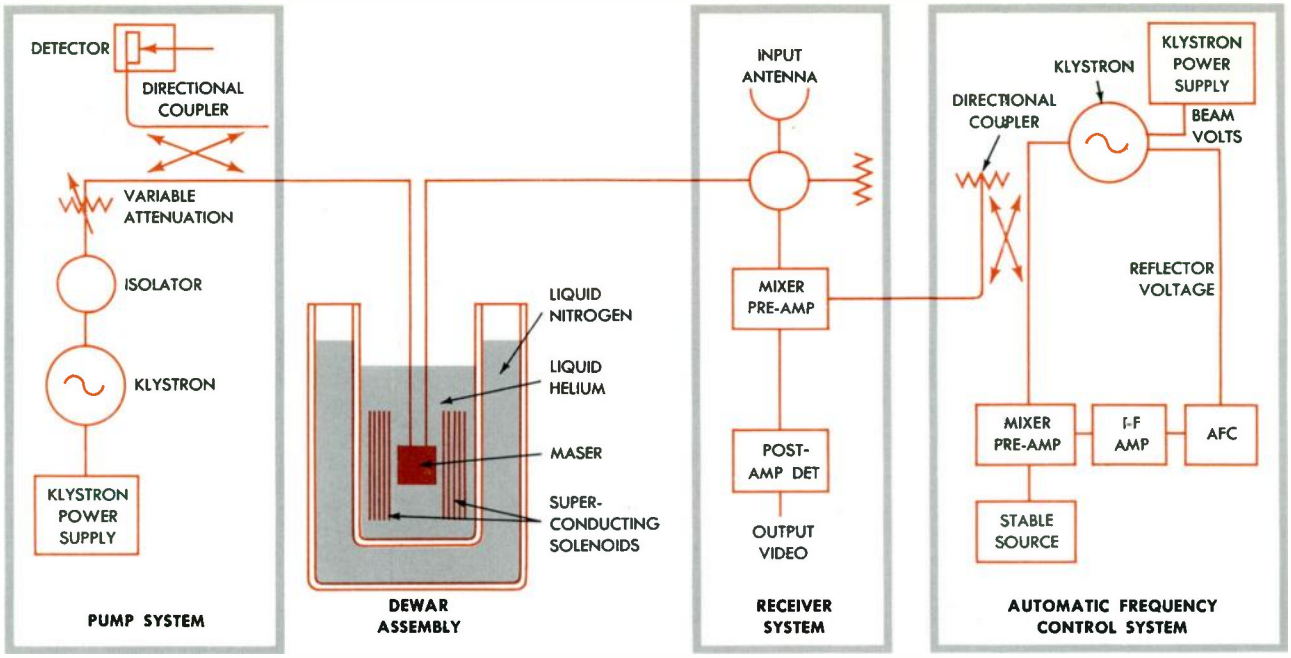

MASER OPERATION has been demonstrated on this two-frequency (65- and 96-kilomegacycle) millimeter wave spectrometer.

five-level maser is the arrangement of the energy levels ($E_3 - E_1 = E_5 - E_3 = E_4 - E_2$) so that a single pumping frequency can pump three transitions simultaneously. This is accomplished by controlling another parameter, a magnetic field that surrounds the maser crystal. This field is used to control the paramagnetic spin energy levels of the maser material.

In the maser demonstrated, the material is the iron ion Fe^{3+}, in a host of TiO_2 (rutile). The energy levels of this maser material, plotted as a function of magnetic field for a particular orientation[1] of the crystal, are shown in Fig. 3. For the crystal orientation selected, a field of 7350 gauss produces the desired equal-energy transitions for a pumping frequency of 65.2 kmc.

Superconducting Solenoid

A low-temperature environment is required for low noise level maser operation; high-field uniformity is required to obtain maximum gain and bandwidth. Both of these requirements can be satisfied by the recently developed superconducting solenoid. The niobium-zirconium superconducting solenoid used in this maser system was designed and built by Westinghouse Cryogenic Systems and produces an 8000-gauss field with a field homogeneity of 2 parts in 10 000. The solenoid consists of a pair of coils as shown in the photograph. The spacing between the coil pairs provides radial access to the magnetic field. The solenoid weighs approximately five pounds and is equipped with a persistent-current switch for operation in the persistent-current mode. During this mode of operation, the superconducting solenoid does not require any external power since the niobium-zirconium wire has zero resistance at liquid helium temperature. In contrast, a conventional 8000-gauss electromagnet would weigh approximately 1200 pounds and would require a continuous power input of three kilowatts.

The resonant cavity consists of a single crystal of iron-doped rutile, 0.05 inches in diameter and 0.049 inches long. Because of the high dielectric constant and low loss tangent of rutile, the material itself can be used as the resonant cavity. Both the cavity and the superconducting solenoid are immersed in a liquid helium bath at a temperature of 4.2 degrees K.

At least 10 db amplification has been demonstrated with the 96-kmc maser. Continued development is expected to yield higher gain with noise figures of less than 2 db—a 16 to 18 db noise figure improvement over existing conventional receiver techniques.

Millimeter Wave Radar

The new maser system is not presently ready for operational use, since hardware development is needed before it can be put into actual equipment. However, maser operation has been demonstrated in a two-frequency (65- and 96-kmc) spectrometer, shown diagrammatically in Fig. 4.

One example of the possible advantages of extremely high signal frequencies now made possible is in the field of doppler radar. Here, higher frequencies can provide a considerable improvement in the detection of slow-moving objects. For example, with 10-kmc radar frequencies, a target must be moving at about 33 knots to provide a doppler-frequency shift of 1 kc; however, if radar frequency is raised from 10 kmc to 100 kmc, the target need only be moving at 3.3 knots to provide the 1-kc doppler frequency. Other possible applications for the new millimeter wave maser are in radiometry and space communications.

[1] "Maser Operation at 96 Kmc with Pump at 65 Kmc," W. E. Hughes *Proceedings of the IRE*, Vol. 50, No. 7, July 1962.

A Selective Load Shedding System

G. D. Rockefeller, *Relay-Instrument Division, Westinghouse Electric Corporation, Newark, New Jersey.*

This selective load shedding relay system preselects expendable feeders for tripping should a tie line or generator be lost, so that proper balance is maintained between remaining local system capacity and remaining loads.

Industrial, municipal, and small utility power systems often depend on a larger electric utility to supply a high percentage of their load. Power is usually supplied to the smaller system over a single transmission line. If this tie line is lost, the smaller system cannot generate sufficient power to carry its full load. In the past, overload on local generation has been prevented by applying underfrequency relays to trip preselected feeders. However, this method is not completely satisfactory because during heavy load periods, insufficient load may be tripped; and during lighter load periods, too much load may be tripped.

To overcome these shortcomings, a more selective load-shedding system has been developed. This new relay system (Type SLS) monitors all sources of power and expendable loads, and automatically selects the proper feeder loads to drop if the remote supply is lost. Shedding is instantaneous when an overload occurs. Immediate action prevents the loss of local generation and avoids costly service interruptions to the more important loads.

SLS System Logic

A simplified logic diagram of the monitoring procedure used by the SLS relay system is shown in Fig. 1. Basically, the procedure consists of continuously adjusting load to be dropped so that power required from the remote source *in excess* of the load selected for shedding is balanced by excess local capacity.

Excess local capacity is found by comparing local generated power with rated local generation capacity; the difference is the excess generation capability. Boiler capacity must also be considered, since boilers in industrial systems usually supply steam to both plant processes and steam turbines. Therefore, the boiler's ability to pick up additional load is also a limiting factor, and the lesser of the two —additional generator or boiler capability—determines how much additional load the local system can pick up if remote power is lost.

Power requirements of the local system in excess of load selected for dropping is found by comparing incoming power with load selected for shedding. The difference must

1

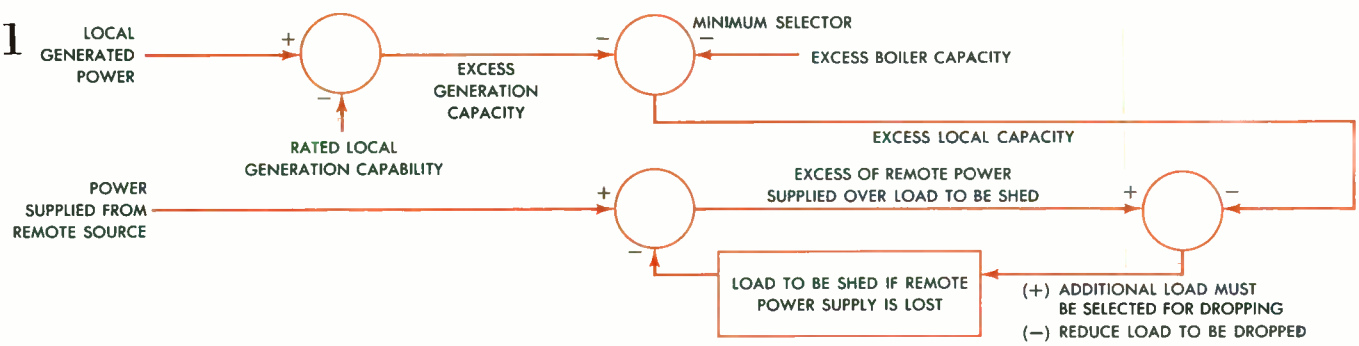

LOGIC DIAGRAM of the selective load shedding system demonstrates the monitoring procedure that is used by the system for determining how many expendable loads should be selected for dropping in case of a tie-line outage.

2

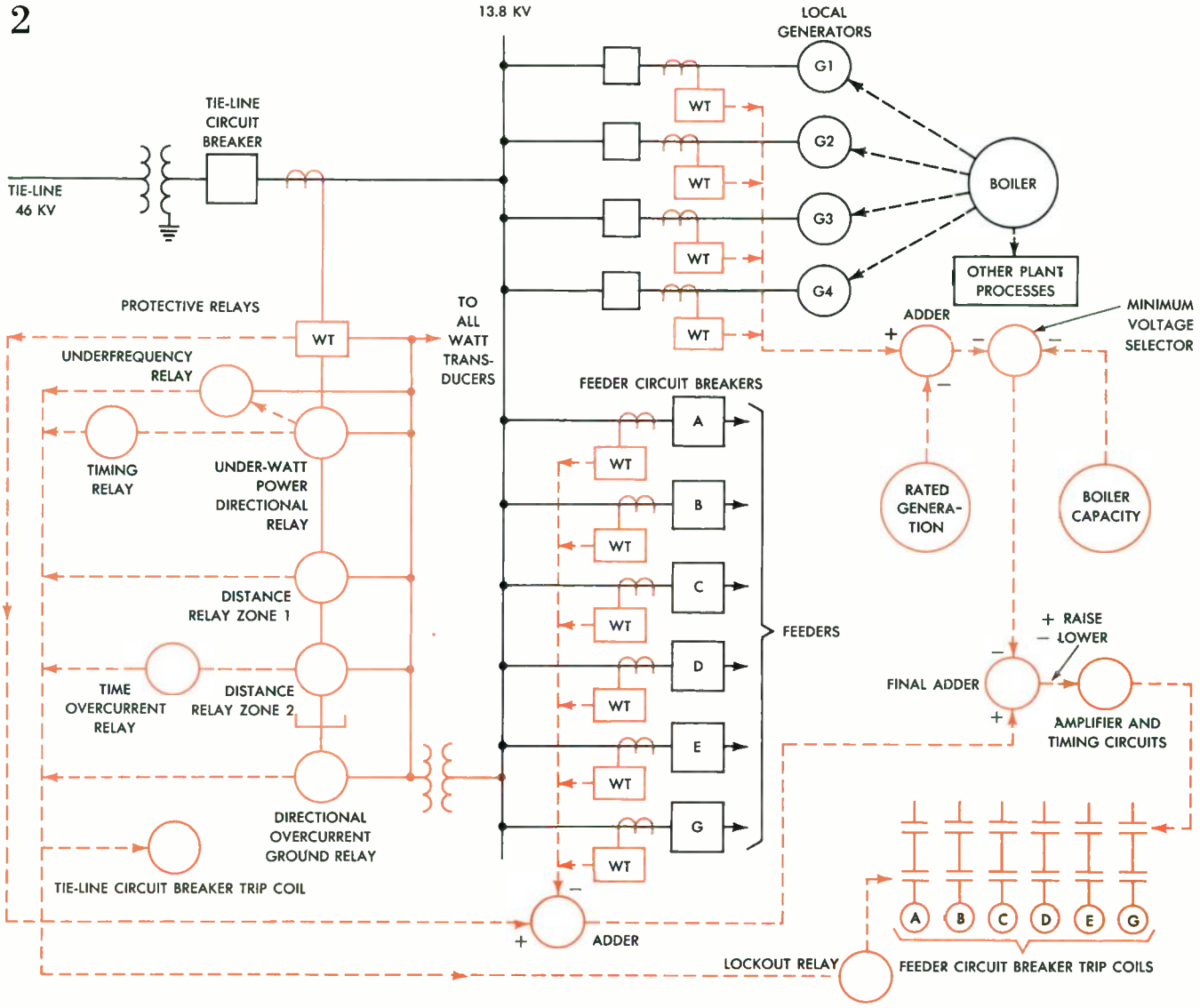

TYPICAL POWER SYSTEM demonstrates the application of the selective load shedding relay system. Watt transducers (WT) provide millivolt signals, proportional to power flow, which are analyzed to determine SLS relay operation. Protective relays provide the tripping signal, which will cause those feeder breakers selected by the SLS relay system to trip.

3

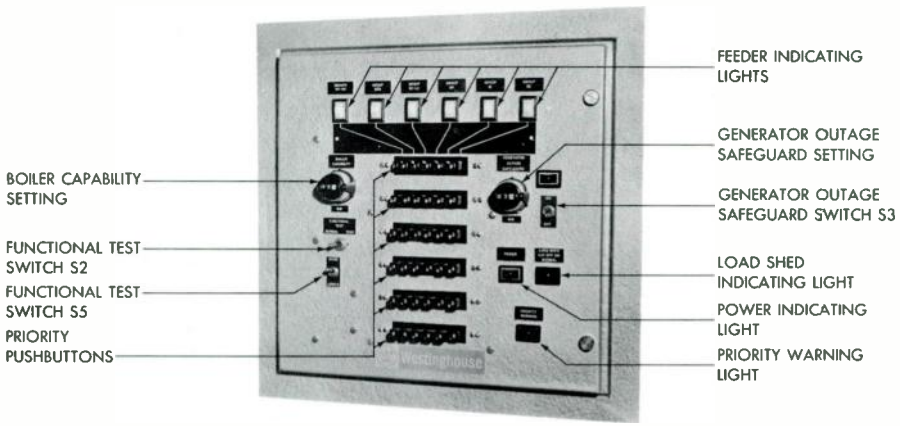

SLS RELAY CABINET contains adjustment settings for the system. The order in which feeders should be dropped or added by the SLS relay is preset on priority selector pushbuttons. Indicating lights tell which feeders have been selected for shedding.

equal excess local capacity. If excess local capacity is insufficient to handle excess power requirements, more load must be selected for dropping; if excess local capacity exceeds excess power requirements, load selected for dropping can be reduced.

SLS relay system operation is accomplished with three major components: (1) Sensing circuitry, which includes watt transducers, potentiometers, and a minimum voltage selector, provides "raise" and "lower" signals; (2) the SLS relay acts upon reception of raise or lower signals to select feeders to be dropped; (3) protective relays initiate instantaneous tripping of the selected feeders when tie-line power is lost. A typical power system shown in Fig. 2 illustrates the application of the SLS relay system.

Sensing Circuits

Sensing circuits compare the various analog signals (proportional to power flows) to determine whether a raise or lower signal is transmitted to the SLS relay amplifier. Generator and boiler capabilities are set on potentiometers. Generator potentiometers (one for each generator) are adjusted so that the total signal is proportional to the total megawatt rating of generators on the line; the difference between this signal and the generator load measured by watt transducers provides an analog signal proportional to the additional load that the generators can pick up.

The boiler potentiometer is set for the boiler's capacity to immediately pick up additional load. The lower of the two quantities—additional load that the generators can pick up, or additional load that the boiler can handle—becomes the additional load capability of local generation, should the tie to the remote power supply be lost.

At the final adder, this additional load capability signal is compared with a signal proportional to the difference between incoming tie line power and feeder loads selected for dropping. (Only selected feeder transducers are energized to provide a signal.)

If additional load capability is less than tie-line excess power, a raise signal is sent to the SLS relay, causing it to select an additional feeder to trip; the selected feeder's transducer is simultaneously energized, which increases the selected feeder circuit signal, and reduces the excess tie-line power signal applied to the final adder. If this action balances the inputs to the final adder, no additional feeders are set to trip.

If tie-line flow is reduced by a reduction in feeder loads, inputs to the final adder become unbalanced; the generation capability signal is now greater, causing the final adder to send a lower signal to the SLS relay. The relay in turn drops out the trip circuit of the last feeder to be picked up for shedding. This feeder's transducer is de-energized, causing the tie-line excess power signal to increase. If the increase is sufficient to balance the final adder, no further raise or lower signal is sent to the SLS relay.

SLS Relay

The order in which feeders are selected to trip by the SLS relay is preset by means of pushbuttons on a priority selector switch (Fig. 3). The SLS amplifier measures the error signal from the final adder circuitry. The relay increases or decreases the feeder circuits to be dropped in the desired sequence until the final adder circuitry is balanced. The SLS relay sets a feeder for shedding by closing a series contact in the feeder breaker trip circuit (Fig. 2). If a protective relay then energizes the lockout relay, the series contacts in the feeder breaker trip circuit controlled by the lockout relay are closed, but only those feeders that have been preselected to trip by the SLS relay are tripped.

A situation may arise where the utility tie line is supplying more power than local generators can pick up even if all feeders under control of the SLS system are set to be shed. In this case the SLS relay activates an annunciator to warn the operator so that he can take appropriate steps, such as starting up another local generator or preparing a feeder that is not programmed in the selective load shedding system for tripping.

Protective Relay Trip Circuits

The tripping signal to the lockout relay comes from outside the SLS relay system. The signal can be provided through underfrequency or reverse-power relays monitoring the tie line. Or if desired, the signal can be provided through auxiliary contacts on the tie breaker.

A typical group of protective relays used to initiate tripping of the tie-line circuit breaker are shown in Fig. 2. Any of these protective relays will not only trip the tie-line breaker but will also energize the lockout relay.

If the tie-line breaker does not trip but the tie line is de-energized by breakers on the remote utility system, the reverse-power relay and the underfrequency relay will trip the local tie-line breaker and the lockout relay. Also, if the tie-line breaker should be tripped manually in error or intentionally, a breaker auxiliary switch contact will energize the lockout relay.

Generator Outage Safeguard

The SLS relay system can remain in service after the utility tie line has been opened to protect against the loss of the largest generator. A generator outage safeguard potentiometer is switched into the sensing circuitry to replace the function of the tie-line watt transducer. This potentiometer is set for the name-plate rating of the largest generator in service, so that feeders are programmed to shed sufficient load upon loss of this generator.

Conclusions

An accurate and instantaneous method for shedding loads on both large and small utility systems is needed. The problem for the large utility is more complex because of the distances between loads to be shed and generation sources. If a large system is overloaded, underfrequency relays selectively shed loads, determined by how much the frequency drops. On smaller systems, such as industrial plants or municipal utilities, the location of loads near generation facilities eases the problem. Feeder loads, generation, and tie-line power can be easily measured, and this information sent to a central location for analysis by the SLS relay system. Where measurement points are remote, inputs may be obtained through telemetering receivers. If breaker locations are remote, transfer-trip functions can be used over pilot channels. With the use of telemetering and transfer-trip schemes, the operating principles of the SLS relay may also be applicable to larger electric utility systems.

Technology in Progress

Test Method Checks Brazed Joints In Electrical Conductors

Brazing is a widely used method for joining electrical conductors, but until recently there has been no simple and convenient way of accurately determining the quality of a brazed joint. Now, however, a convenient shop method has been devised for nondestructive testing.

An ac voltage is applied to the brazed conductor through two sets of probes. One set bridges the brazed joint; the other set spans an equal distance on the conductor itself. The voltage drops across the pairs are differentially compared, and a meter indicates the net difference. The equipment can be made small enough to be carried easily, so the technique is suitable for many quality-control checks.

The new method was devised by transformer engineers, and they have determined experimentally what constitutes a sound brazed joint. In hundreds of tests, the device has been able to detect joints that were poorly bonded for a variety of reasons, ranging from insufficient temperature to too short a brazing time. Efforts to fool the machine by offering it joints with deliberately concealed defects have invariably failed.

The result of this experimentation is an easily used method for checking the quality of brazed joints. Although the measurements are electrical, the result is a good indication of the mechanical strength as well as the conductivity of the joint. ■

Fast Infrared Lenses Designed by New Method

Infrared sensing and viewing systems have become increasingly important for industrial, scientific, and military applications. Such systems can "see" much that is not directly visible by collecting the invisible heat waves radiated by every object in the universe above the temperature of absolute zero.

A major technical problem has been provision of good lenses for collecting and focusing infrared rays. Infrared lenses have been limited by low speed, bulkiness, and poor image quality. Now, to a large extent, these limitations can be overcome by a lens design method that employs a computer to optimize the design variables for a specific lens system.

The method has been used to produce a compact, high-speed, high-resolution infrared lens system. The new system is rated at f/0.75, considerably faster than the typical speed of f/1.5 for previous lenses. It is designed for imaging of infrared radiation with wave lengths from 8 to 12 microns, the so-called far infrared part of the spectrum. This range is of special interest because radiation in it can pass through the earth's atmosphere without being absorbed. Consequently, it constitutes a window for such uses as infrared mapping of the earth's surface by a satellite and infrared communication with space vehicles.

The lens system has three elements. Two are made of germanium, which is transparent to infrared. The third, located between the other two, is made of a synthetic inorganic material known as Irtran-2.

The lens system was designed by feeding its optical requirements into an electronic computer that was programmed for optical design by a technique devised at Massachusetts Institute of Technology. Essentially, the computer program instructs the machine to vary the physical changes that can be made in a lens system—such as lens curvatures and spacings—and compare the images that would result with those that would be produced by an ideal lens system. By this trial and comparison, conducted at very high speed, the computer determines the lens structure that will have the best performance and the fewest optical defects. ■

70-Kmc Traveling-Wave Maser Uses Superconducting Magnet

A traveling-wave maser has been built to operate at 70 kilomegacycles (10^9 cycles per second), a frequency twice that of any previous traveling-wave maser. The maser's pumping frequency is 118 kilomegacycles, and gains of more than 20 decibels at 10-megacycle band-width have been achieved. The device will be used to study advanced radiometers, radar, and communications equipment.

Temperatures approaching absolute zero are required for high-frequency amplification with low noise, so the iron-doped rutile (titanium dioxide) maser element is cooled by liquid helium to 4.2 degrees K. This is in the temperature range at which superconducting magnets operate, so such a magnet is used to produce the applied field.

The niobium-zirconium superconducting magnet produces a 5000-gauss field having a deviation of less than one gauss perpendicular to the 1.5-inch length of the maser element. It weighs approximately three pounds and has a switch for disconnecting the battery power supply to operate in the persistent mode. (In this mode of operation, the magnet operates without any external power supply since the wire has no resistance.)

The magnet was conservatively designed in that nearly twice the required field can be obtained with useable uniformity. The same basic magnet can be extended in length to accommodate rutile elements up to a foot long. The magnet proper fits into a cylinder 3.5 inches in diameter.

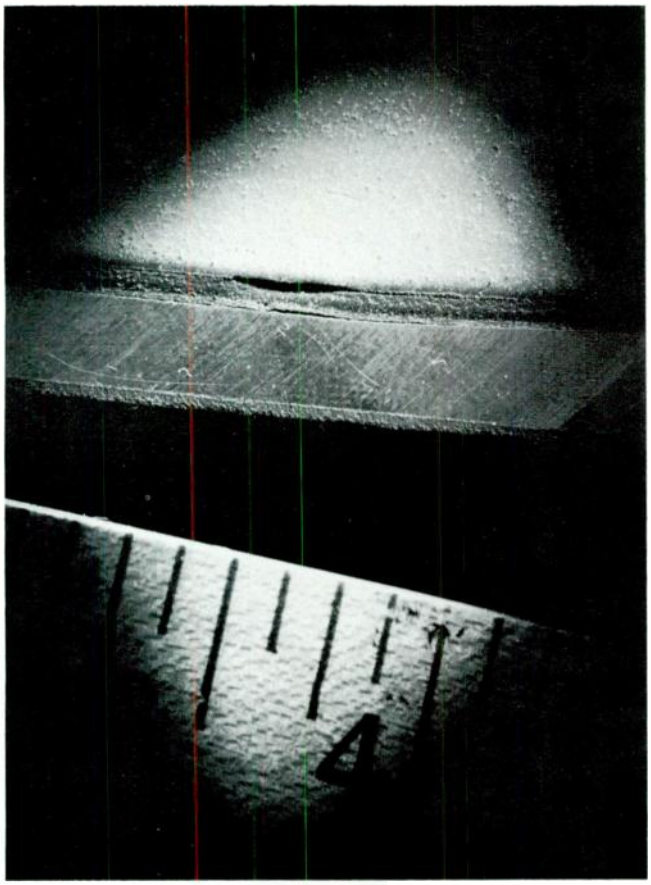

THE CORONA INSPECTION METHOD detects hidden defects such as this one (revealed by sectioning a structure of rubber bonded to metal).

Since there is no resistance in the magnet wire at liquid-helium temperature, there is no heat loss. This is a great advantage in this application because the maser element must be kept at very low temperature. While a conventional electromagnet would require only about 20 watts to produce the required field, the heat loss from even this amount of power would be too great because it would cause rapid loss of liquid helium. If a closed-cycle refrigeration system were used to carry off the heat, the maser system's cost, size, and weight would be excessive.

Other advantages of using a superconducting magnet include substantial reduction in size and weight, high field uniformity and intensity, and ability to disconnect the battery power source. The magnet also provides tuning for maser operation because its field can be varied. Once the selected value is reached, the magnet can be operated in the persistent mode. This assures high field stability and also makes the unit portable.

The 70-kmc maser was developed for the U. S. Army Electronic Research and Development Laboratory, Fort Monmouth, New Jersey. ■

Nondestructive Inspection Method Employs Corona Measurement

Detection of corona discharges is a useful way of locating flaws in electrical insulation, and it has now been adapted for nondestructive inspection of other materials. The inspection method uses the principle that gas-filled spaces in or adjacent to solid nonconducting materials ionize when a high voltage stress is applied across the material. The method can be applied to virtually any dielectric material and any shape of object, provided the thickness is not more than one to two inches in the region that is to be tested.

Electrodes are applied to two sides of the object, and an ac potential from a high-voltage transformer is connected to the electrodes. The voltage is adjusted to the level required to ionize the gas in any voids in the material. Ionization of the gas in a void causes pulses of high-frequency current in the high-voltage circuit. These pulses are amplified and measured by a detector circuit connected to the high-voltage circuit.

The type of inspection desired determines the manner in which the method is applied. If it is only necessary to determine whether or not flaws are present, large-area electrodes are used to test all, or a large part, of the object at one time. If the *location* of flaws has to be determined, the object is scanned with a small electrode.

The latter approach has been used successfully to locate flaws in structures made of rubber bonded to metal. Two

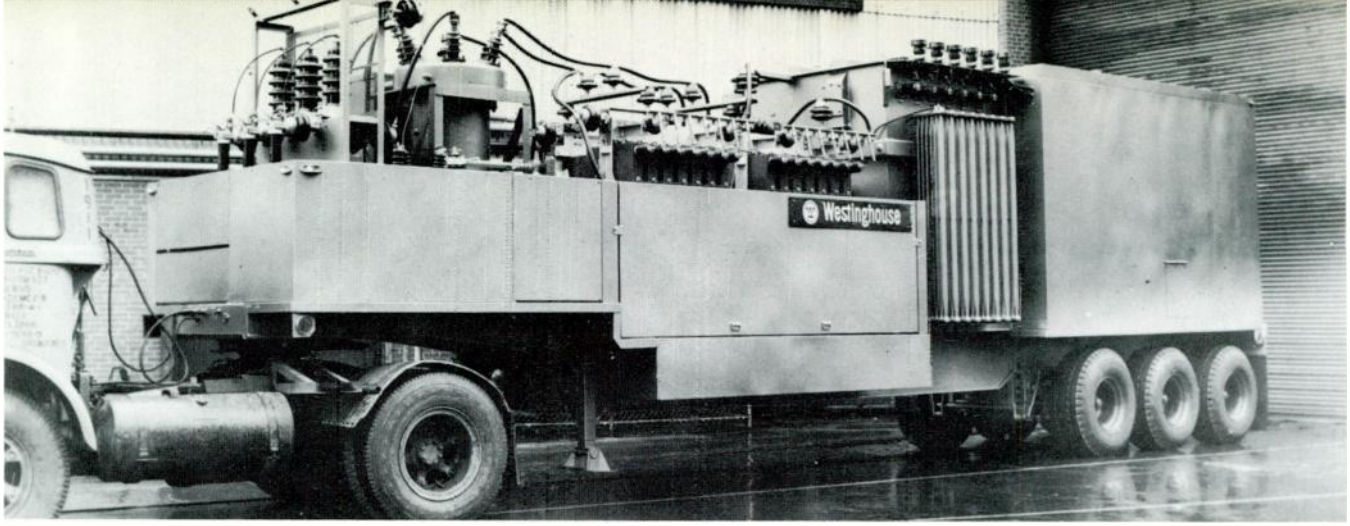

THIS 40-FOOT MOBILE CONVERTER is for the NEAR (National Emergency Alarm Repeater) system being evaluated by the Department of Defense, Office of Civil Defense. In operation, the unit would superimpose a 210- or 270-cycle signal voltage on a conventional utility distribution system. This would actuate frequency-sensitive receivers plugged into home outlets.

The 50-kva unit includes high-voltage lightning arresters, fuses, breaker and coupling capacitors. 60-cycle shunt reactor and series tuning reactor, rectifier transformer and necessary output filters, and a 210- or 270-cycle inverter. Three lines connect the converter to the high-voltage system. The unit was built by the Westinghouse Power Transformer Division, and field tests are under way on the Columbia Water and Light Department's system in Columbia, Missouri.

types of flaws were present—gas bubbles within the rubber and lack of bonding between the rubber and metal inserts. (See photograph.) The inspection process was automated by programming the movement of the small scanning electrode and by applying the signals from the detector circuit to a recorder that mapped the location and size of defects.

The test method can be used with any nonconductor capable of withstanding the required voltage stress. This comprises most plastics, plastic laminates, rubbers, ceramics, glasses, and glass-fiber filament-wound structures. The objects can be flat or curved, smooth or rough. Both sides of the material must be accessible to an electrode, which can be a conducting liquid such as water on one or both sides. If the material is bonded to a conducting metal, the metal can serve as an electrode.

Voids as small as 0.001 inch across can be detected. The sensitivity and the voltage level required vary with such conditions as the dielectric constant of the material, the size and shape of any voids present, and the gas pressure in the voids.

Products for Industry

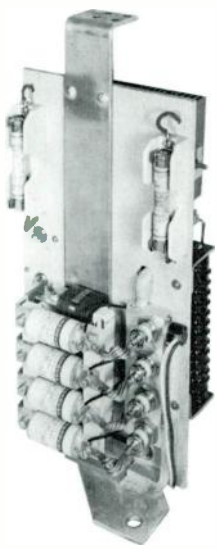

SILICON DIODE ASSEMBLIES are sized and rated to replace ignitron-tube sections of industrial rectifiers. Advantages include simplicity, higher efficiency, longer life, less maintenance, smaller space and cooling-water requirements. The assembly includes diode current-limiting fuses, balancing reactors, neon indicating lamps, and over-temperature thermostats. *Westinghouse Rectifier Product Line Group, East Pittsburgh, Pa. 15112.*

TWO-SPEED INDUSTRIAL DRIVE MOTOR (400 rpm and 3450 rpm) can be reversed up to four times a minute. It is manufactured on a NEMA 56 frame and rated one-half and one-quarter horsepower at 230 volts single phase, 208 volts polyphase. It can be belt connected or directly connected to a machine, eliminating the need for a speed-change transmission. The Dual Drive motor's low-speed winding is of permanent split-capacitor design, which is especially suited for frequent reversing. High-speed winding is of capacitor-start type. *Westinghouse Small Motor Division, Lima, Ohio 45801.*

QUARTZ-CRYSTAL MICROBALANCE measures evaporated, sputtered, or chemically deposited films from 0.05 to 40 000 angstrom units thick, with an accuracy better than one percent. One of two crystals in the unit is exposed to the deposition source, and the other protected. The exposed crystal's frequency (which decreases in proportion to the mass deposited on it) is mixed with that from the reference crystal, and the resulting beat frequency represents film thickness. The instrument can be used while processing. *Westinghouse Scientific Equipment Department, Pittsburgh, Pa. 15235.*

STATIC CONTACTORS for heavy-duty industrial applications have logged more than 8 000 000 operations and 22 000 hours of uninterrupted maintenance-free service in initial installations. Controlled rectifiers are the switching elements in these Trinistrolcontactors. Ratings range from 7.5 to 100 horsepower in various voltages and frequencies. Signals from computers, photo cells, limit switches, and thermocouples can be used to energize the controlled-rectifier gates. *Westinghouse General Control Division, Buffalo, N.Y. 14205.*

About the Authors

C. G. Helmick has been a frequent contributor of Westinghouse ENGINEER articles on industrial drive and control systems. He joined Westinghouse on the graduate student course in 1951 and was assigned to the general mill section, industrial engineering department (now the Processing Province, Industrial Systems). Most of his time is devoted to development and application of drives and controls for the chemical fiber industry.

Helmick earned his BSE in electrical engineering at the University of Michigan in 1950 and his MSE the following year. He has since taken graduate work in business administration at the University of Pittsburgh.

Kenneth Lipman is a new writing teammate for Helmick, and a new author in the ENGINEER. He came to Westinghouse in 1956 after experience in instrumentation design with A. B. DuMont Laboratories and the U. S. Bureau of Mines. He served first in the director systems department, where he designed proximity switches and temperature control systems. Lipman moved to the General Control Division in 1960 and there has worked on design and test of firing circuits, static starters, dc chopper converters, regulated dc power supplies, and inverters. He is now a senior design engineer in the static power equipment product group, responsible for design of variable-frequency inverters.

Lipman graduated from Carnegie Institute of Technology in 1946 with a BS in electrical engineering. He earned his MS in electrical engineering in 1953 at the University of Pittsburgh.

Since joining Westinghouse on the Graduate Student Program in 1922, **S. B. Griscom** has been associated with almost every phase of electric utility engineering, and particularly with high-voltage transmission systems.

His first assignment was with the high-voltage and impulse-voltage laboratories. In 1924, he joined the general engineering department, which is now the electric utility engineering department. Here, Griscom has worked as a development engineer, a sponsor engineer working directly with electric utilities, and an advisory engineer working on a variety of high-voltage transmission projects. He is presently a Consulting Engineer, and although his attention is now mostly centered on lightning studies, he is often called on to help with almost any problem that involves electricity.

Griscom's participation in his field is appropriately summarized by the *AIEE William M. Habirshaw Award*, which he received in 1961 for ". . . outstanding contributions to the development and application of improved lightning and short-circuit protection of electric power systems, and high voltages for commercial and residential area distribution."

Griscom is a graduate of Cornell University with the degree of Electrical Engineer.

R. K. Riel is an oldtimer in the young semiconductor technology. He started in 1948 with Eagle-Picher Company, where his work included research in production methods for germanium and silicon, studies of the properties of semiconductor materials, preparation of cadmium-sulfide solar cells, germanium-film gas detectors, and silicon films for large-area solar cells. He moved to Minneapolis-Honeywell in 1957 and participated in studies of horizontal crystal growth, etch pits, and other investigations. Riel joined the Westinghouse Semiconductor Division in 1959 and is manager of the special products engineering department, a department that is concerned primarily with the development of improved solar cells.

Riel received his BA in mathematics at Northeastern State College, Oklahoma, in 1948. He later did work in electrical engineering and advanced mathematics at the University of Arkansas and Kansas State College of Pittsburg (Kansas). He is a member of the American Physical Society and the Electrochemical Society.

K. S. Tarneja earned his BSc degree in physics at Delhi University, India, in 1952 and his BSc in mechanical engineering at Benares Hindu University in 1956. He worked as a mechanical engineer in India and then came to the United States in 1957 to enter Carnegie Institute of Technology. He received his MS in mechanical engineering in 1958 and has since done graduate work in metallurgy. He will earn a master's degree in business administration at Duquesne University late this year.

Tarneja joined the Westinghouse Semiconductor Division in 1959. He performs research and development work on high-efficiency solar cells, a field that has taken him into the investigation of diffusion problems and also into the design, fabrication, and testing of cells.

George D. Rockefeller graduated from Lehigh University with a BSEE in 1948. He joined the Westinghouse relay-instrument division in 1951 after working for the Metropolitan Edison Company. Presently a General Engineer in the relay-instrument division, Rockefeller has spent most of his working time designing and applying protective relaying systems. Although this is his first appearance in the ENGINEER, he has authored some two dozen technical papers and articles on the subject.

Rockefeller is a Senior Member of IEEE and holds a Professional Engineer's License in New Jersey.

The description of the UK-2/S-52 International Satellite Program in this issue is provided by **Emil W. Hymowitz,** NASA Project Manager for the program, and **Harold M. Watson,** Project Manager for Westinghouse activity in the program.

Hymowitz graduated from the University of Maryland in 1950 with a BSEE. He worked as a test equipment designer at the Baltimore Signal Depot until 1951, when he was transferred to the Naval Air Test Center at Patuxent River. Here, as Project Engineer and Unit Head, he conducted airborne equipment evaluation, primarily of radar and countermeasures systems. In 1956, Hymowitz moved to the Navy Department, Bureau of Aeronautics, where he headed the Surveillance Section of the AEW and Control Branch. He was responsible for initiating and coordinating Navy research and development efforts in the area of airborne early warning radar and counter-countermeasures systems.

Hymowitz was appointed to his present position of NASA Project Manager for the UK-2/S-52 International Satellite Program in March 1961. He has primary responsibility for detailed project planning and execution from project initiation until the satellite has been launched and all available experimental and engineering data have been reported.

Watson graduated from the University of Colorado with a BSEE in 1943. He joined Westinghouse, and went to work in the Special Products Division and Central Engineering Division. Assignments during this period included developmental work on steam turbine governors for shipboard use, tie-line load regulators, a bomber sight, wing vibration testing equipment, fire control computers, radar antenna drives, and automatic pilots. In 1949, he was made manager of the Electromechanical Section and was responsible for a variety of electromechanical projects and controls for aircraft and missile applications. When the Air Arm Division was formed in 1951, Watson became manager of the Electromechanical Techniques Section and continued to work on aircraft and missile applications.

In 1958, Watson was made manager of the Support Equipment and Instrument Sections. Watson became Project Manager for the UK-2/S-52 Satellite Project, his present position, in 1962.

Molecularized TV

This developmental television camera is intended for such space applications as lunar reconnaissance, satellite inspection, or observation of orbiting astronauts or equipment. The 27-ounce camera (without lens) is seven and one-half inches long, two inches wide, and three and one-quarter inches deep. It requires 50 cubic inches of space and four watts of power. The light weight, small size, and low power requirements have been accomplished with the help of molecular electronics, the concept that integrates into tiny blocks of solid materials functions ordinarily performed with assemblies of electronic components. There are 197 components in this molecularized television camera, including 36 molecular electronic blocks; if conventional circuitry and components were used in an equivalent television camera, 582 individual components would be required.